INL/RPT-23-74687

Corrosion Testing Needs and Considerations for Additively Manufactured Materials in Nuclear Reactors

September 2023

Andrea Jokisaari[1], Yiren Chen[2], Thomas Hartmann[3], Vineet Joshi[3],
Isabella van Rooyen[3], Rongjie Song[1], and Jonathan Wierschke[3]

[1]*Idaho National Laboratory*
[2]*Argonne National Laboratory*
[3]*Pacific Northwest National Laboratory*

INL/RPT-23-74687

Corrosion Testing Needs and Considerations for Additively Manufactured Materials in Nuclear Reactors

Andrea Jokisaari[1], Yiren Chen[2], Thomas Hartmann[3], Vineet Joshi[3],
Isabella van Rooyen[3], Rongjie Song[1], and Jonathan Wierschke[3]

[1]Idaho National Laboratory
[2]Argonne National Laboratory
[3]Pacific Northwest National Laboratory

September 2023

Idaho National Laboratory
Idaho Falls, Idaho 83415

http://www.inl.gov

Prepared for the
U.S. Department of Energy
Office of Nuclear Energy
Under DOE Idaho Operations Office
Contract DE-AC07-05ID14517

Page intentionally left blank

SUMMARY

The Advanced Materials and Manufacturing Technologies (AMMT) program within the Department of Energy, Office of Nuclear Energy (DOE-NE) has developed its current recommendation for its corrosion testing strategy to deploy additively manufactured (AM) materials in advanced nuclear reactors. Additive manufacturing technologies have developed rapidly in recent years, creating new opportunities and challenges for the nuclear industry. To adopt AM technologies, the corrosion performance of AM materials needs to be adequately evaluated.

This document is divided into seven chapters designed to support the proposed corrosion research strategy. The strategy focuses on the testing of AM 316H stainless steel (SS) to align with the broader AMMT program. An overview of localized and uniform corrosion mechanisms and their synergy with other degradation modes is provided. Specifically, the corrosion resistance of 316H is largely provided by the presence of an intact chromium oxide film on the surface, and loss or damage of this film is generally responsible for corrosion degradation. Engineering concerns for corrosion behavior are discussed, including component failure mechanisms and corrosion codes and standards. While the standards are extensive, certain material testing standards do not exist that would be relevant for the AMMT program. Reactor-specific corrosion concerns for molten salt reactors, liquid metal-cooled reactors, and high-temperature gas reactors will guide corrosion testing. Key factors likely to influence corrosion properties of AM materials (especially 316H) include build porosity, the presence of unusual phases, residual stress, microsegregation within the cellular substructure, and surface roughness. Post-build treatments and process variability need to be assessed with multiple specimens that are microstructurally quantified to develop structure-property-performance relationships with uncertainty quantification. Sufficient facilities exist, at least for initial program efforts focusing on characterization of unirradiated material in laboratory settings, across Argonne National Laboratory (ANL), Idaho National Laboratory (INL), Oak Ridge National Laboratory (ORNL), and Pacific Northwest National Laboratory (PNNL).

The recommended path forward segments the complex nature of additively manufactured material microstructures, as-built component surfaces, and advanced reactor environments. The AMMT program will initially focus on the experimental characterization of AM 316H corrosion by molten chlorides and liquid sodium. With additional time and resources, molten fluorides, high-temperature helium, liquid lead, and other advanced reactor environments will be studied, in that order, as will other materials. Light water reactor environments will not be studied, as they fall under the scope of the Light Water Reactor

Sustainability program. Given the complexity of AM material microstructures and their interplay with corrosion mechanisms, an experimental campaign is initially recommended.

Testing unirradiated specimens in a laboratory environment is recommended as the first step. The second stage of corrosion testing for reactor environments should entail *ex situ* testing of irradiated AM material to determine the impact of irradiation-driven microstructural changes on corrosion behavior. Finally, depending on the availability of testing capabilities, *in situ* corrosion testing can follow, exploring possible transient effects induced by irradiation, coolant flow, or temperature gradient.

Corrosion testing will characterize phenomena of engineering interest and explain corrosion mechanisms at the mesoscale. The specific corrosion testing strategy employed for a given reactor environment will depend upon the degree of prior knowledge about the behavior of the material composition in that environment. Because AM components may be deployed without further surface finishing, understanding the effect of the surface on corrosion behavior is crucial. Build porosity is also a concern, as is the presence of oxide phases or atypical inclusions and residual stresses. Given the likelihood of crevice corrosion on the as-built surface, three-dimensional non-destructive examination before and after corrosion testing is recommended, such as X-ray computed tomography. Conversely, as-built specimens finished to a smooth surface may be useful to assess underlying corrosion mechanisms and understand the extent to which corrosion is localized to or affected by the rough surface. Thus, a given material should be tested with both the rough surface and a polished surface. The corrosion assessment may also include conventionally manufactured (e.g., wrought) smooth specimens of the same composition.

Process variability, including geometry of the as-built specimen from which corrosion samples are removed, should be addressed with a combination of experiments and data analytics. Variability should be considered at the microscale and the macroscale. At the microscale, the statistical distribution of a corrosion behavior of interest should be understood with respect to key microstructural features. Conversely, macroscale variability can be tested by taking samples from different locations within a component.

For maximum impact, the materials tested within the AMMT corrosion campaign must be the same as the materials employed within the neutron irradiation, ion irradiation, and rapid qualification testing. Coordination is required across program areas to ensure sufficient material with a fully traceable pedigree is available for testing.

ACKNOWLEDGEMENTS

This work was sponsored by the U.S. Department of Energy, Office of Nuclear Energy, Advanced Materials and Manufacturing Technologies program. This manuscript has been authored in part by Idaho National Laboratory, operated by Battelle Energy Alliance, LLC under Contract No. DE-AC07-05ID14517; by Argonne National Laboratory, managed and operated by UChicago Argonne LLC, under Contract No. DE-AC02-06CH11357, and by Pacific Northwest National Laboratory, operated by Battelle Memorial Institute under Contract No. DE-AC05-76RL01830.

Page intentionally left blank

CONTENTS

FIGURES

TABLES

ACRONYMS

AM	additively manufactured
AMMT	Advanced Materials and Manufacturing Technologies
ASME	American Society of Mechanical Engineers
DED	directed energy deposition
DOE	Department of Energy
EAC	environmentally assisted cracking
EB	electron beam
F/M	ferritic-martensitic
HTGR	high-temperature gas-cooled reactor
IASCC	irradiation-assisted stress corrosion cracking
LAS	low-alloy steels
LFR	lead-cooled fast reactor
LMD	laser metal deposition
LME	liquid metal embrittlement
LPBF	laser powder bed fusion
LWR	light water reactor
NE	Office of Nuclear Energy
NRC	Nuclear Regulatory Commission
ODS	oxide dispersion strengthened
PM-HIP	powder metallurgy–hot isostatic pressing
SCC	stress corrosion cracking
SFR	sodium-cooled fast reactor
SLM	selective laser melting
SMR	small modular reactor
SS	stainless steel

Page intentionally left blank

1. INTRODUCTION

1.1 Goal of the Report

This document aims to discuss the corrosion testing needs and considerations for additively manufactured (AM) materials to be deployed in nuclear reactors and to develop the corrosion research strategy for the Department of Energy (DOE) Office of Nuclear Energy (NE) Advanced Materials and Manufacturing Technologies (AMMT) program for fiscal year 2024–2026. The AMMT program will develop cross-cutting technologies in support of current fleet and next-generation advanced nuclear reactor technologies and maintain U.S. leadership in materials and manufacturing technologies for nuclear energy applications. The overarching vision of the AMMT program is to accelerate the development, qualification, demonstration, and deployment of advanced materials and manufacturing technologies to enable reliable and economical nuclear energy [1]. While the AMMT program scope has recently expanded to include conventionally manufactured materials, this report is focused on the specific concerns of corrosion for AM materials, being a novel research area with unique issues. This report will provide a comprehensive review of AM corrosion behavior to support understanding of the current state-of-the-art of the field and to identify the research needs and strategies related to corrosion of AM materials for nuclear applications. The objective is to develop a knowledge base of research activities and testing capabilities to characterize the environmental effects (specifically, corrosion effects) of AM materials. The outcome of this work will help determine the basic needs and concerns specific to the corrosion of AM materials for structural applications in reactor conditions and support future AMMT efforts for determining the corrosion responses of new AM materials for reactor environments.

This report is generally constrained to a focus on 316 stainless steel (SS), although the AMMT program is researching several other metallic alloy systems as well, including nickel-based alloys and refractory alloys. Constraint of the discussion to AM 316 SS serves two purposes: (1) many of the concepts described in this report can be applied to other metallic alloys as well, and (2) the AMMT program has chosen to demonstrate its accelerated qualification and deployment framework on AM 316 SS [1]. This material was chosen for its relevance to multiple advanced reactor technologies and the existing qualification of conventionally manufactured 316 SS in the American Society of Mechanical Engineers (ASME) code. As a result, AM 316 SS is currently the highest priority for corrosion studies within the AMMT program; other materials can also be studied as additional resources are made available.

The focus of the AMMT program to develop and demonstrate a rapid qualification framework to be used by industry drives the development of the corrosion research strategy within this report. The goal of the corrosion research within the AMMT program is to assess the macroscopic and mesoscopic corrosion behaviors of AM material to enable the deployment of the material into advanced reactors. As a result, different advanced reactor environments must be considered along with the possible corrosion-induced failure modes of the material. In addition, a large body of information exists for certain material compositions (e.g., 316 SS) that are conventionally manufactured. A significant aspect of the investigation will be the determination of how additive manufacturing processes affect the corrosion behavior for a given material composition versus its conventionally manufactured analog. Given the available resources and the focus of the AMMT program, the proposed corrosion research strategies within the report will be limited to experimental investigations excluding significant advanced modeling and simulation.

1.2 Background on Metal Additive Manufacturing

Metal additive manufacturing holds significant promise as an enabling technology for the 21^{st}-century nuclear energy industry. Metal additive manufacturing can fabricate novel materials and innovative component designs that are not achievable through conventional manufacturing, such as forging or machining. By making components in a layer-by-layer fashion, AM technologies enable the fabrication of components with complex geometries with minimal waste. Hearkening back to the origin of AM as a rapid prototyping technology, components are manufactured directly from computer-aided design models without the production of tooling. This also makes AM technologies inherently more flexible and less expensive than traditional manufacturing processes for limited production runs. Components can be fabricated as net-shape or near-net-shape, in which the as-built surface finish is retained in the component, or removed via final machining, respectively. Net-shape fabrication reduces manufacturing cost by removing the final machining step; however, the surface roughness of the component is generally on the order of the size of the feedstock used for fabrication and must be acceptable for the service of the component.

The rapid development of additive manufacturing technologies in recent years has impacted many industrial sectors [2, 3]. Successful applications of AM technologies with improved performance and competitiveness can be found in a wide range of engineering fields, from automotive [4] to aerospace [5] industries. Metal additive manufacturing has even been deployed by the United States Navy for the fabrication of reactor door hinges [6]. Likewise, AM technologies also create new opportunities for the nuclear industry [7]. Numerous pilot programs to employ AM technologies for current operating nuclear power plants and future advanced reactors have emerged [8, 9]. The unique advantages of AM technologies have the potential to transform the nuclear industry with innovative material and manufacturing solutions [1].

Alongside the emerging opportunities for the nuclear industry, the introduction of AM technologies also presents new challenges. Materials and components produced with AM technologies possess different defects, microstructures, and internal stress states in comparison with traditionally produced materials. Consequently, the properties and service performance of AM materials can be significantly different from their traditionally fabricated counterparts. Preliminary research on AM materials focusing on light water reactor light water reactor (LWR) applications [10, 11] has shown some promising results. The performance and degradation of AM materials can be similar to that of traditional materials and can be understood with the existing degradation mechanisms. Nonetheless, little information is available on how AM materials will perform in advanced reactor environments [12, 13]. Some characteristics of AM materials, such as dislocation cells, micron-scale pores, and mesoscale compositional heterogeneity may be critical for their performance in advanced reactor environments where high operating temperatures, challenging chemical environments, and high neutron fluxes and fluences are anticipated. To fully realize the benefits of AM technologies, the unique characteristics of AM materials must be understood and their impacts on in-service performance must be evaluated.

Multiple AM technologies have been developed in recent years which may fundamentally alter the component design and supply chain in the nuclear industry. Key AM technologies deemed relevant to nuclear reactor core structures are laser powder bed fusion (LPBF), laser directed energy deposition (DED), powder metallurgy–hot isostatic pressing (PM-HIP), electron beam (EB) welding, and cold spray [14]. These technologies are not currently in widespread use, but they have the potential to drastically reduce fabrication costs, timelines, and quality assurance burdens as well as to access new component geometries and materials properties not achievable by conventional manufacturing [15]. Some of the most common metals available for additive manufacturing include stainless steels, nickel, cobalt-chrome, titanium alloys, and aluminum. Expanding this selection of feedstocks and developing AM printing methods promise to increase the flexibility of materials engineers and address the needs of nuclear technologies in the 21st century.

Metal additive manufacturing techniques can be classified by the metal joining method, including lasers, nozzles, and electron beams. Some of the benefits of AM processes include no specialized tooling and less material waste. Depending on the technique employed, the resulting printed part may be net-shape (requiring no machining) or near-net shape (requiring final machining to achieve, e.g., dimensional tolerances or a given surface finish). Because AM is a layer-by-layer fabrication process, the finally obtained physical object possesses step features. A thinner layer thickness improves surface finish but increases building time. Besides layer thickness, many other processing parameters exist, including heat power, traveling speed, material feed rate, and hatch spacing [16]. Below are some of the most common metal additive manufacturing techniques.

Metal powder bed fusion involves the selected melting of a layer or bed of metal powder to create a component [15, 17]. After creating one layer, additional powder is deposited in the bed via rollers or blade and the build is continued. Energy deposition occurs via laser beam or electron beam, and specific methods include electron beam melting, direct metal laser sintering, selective heat sintering, and selective laser melting. The most commonly employed metals in this additive process are stainless steel, titanium, aluminum, steel, and cobalt chrome, and copper. Powder bed fusion methods typically result in work pieces with relatively fine surface finishes and with the largest dimensions on the order of 30 cm.

Directed energy deposition (DED) is similar to laser powder bed fusion in that a directed energy source, such as laser beam or electron beam, is rastered in the process of building the component [15, 17]. However, directed energy deposition methods involve the simultaneous rastering of feedstock material with the energy source, and metal feedstock material can be either powder or wire form. DED methods can be used to repair existing components as well as to manufacture large-scale components due to their fast build rates. However, surface finishes are typically much rougher than those achieved from powder bed fusion methods.

Powder metallurgy-hot isostatic pressing (PM-HIP) and cold spray are considered advanced manufacturing methods by the U.S. Nuclear Regulatory Commission (NRC) [14]. Although not considered additive manufacturing for these purposes, they are briefly described here. PM-HIP involves the sintering of metal powders to create components and is typically employed when melting a metal powder is impracticable (e.g., refractories) or would adversely impact material properties. The material is consolidated under both isostatic pressure and heat, resulting in components with very little porosity. Cold spray is a method to deposit coatings onto substrate materials by entraining powders in supersonic gas, resulting in the plastic deformation of the powder when it impacts the substrate.

As-fabricated AM components are characteristically different from conventionally manufactured components both in terms of microstructure and as-fabricated surface finish [18] due to their very different fabrication methods. While additively and traditionally manufactured materials can be compositionally similar, their corrosion behaviors can be different because both AM microstructures and AM surface finish may play critical roles in corrosion. Due to the high cooling rate and rapid solidification commonly associated with AM technologies, AM materials often exhibit dendritic microstructures and high-temperature phases that have significant impacts on their corrosion resistance [19]. Porosity, residual stress, and surface roughness are also known to have detrimental effects on corrosion behavior [20, 21]. Furthermore, post-build heat treatments alter the AM microstructure, giving rise to a wide range of secondary phases or precipitates, which could also have significant consequences on the material's corrosion responses.

1.3 Overview of Advanced Reactor Environments

Within the nuclear industry, a broad spectrum of reactor environments exist, ranging from high-temperature water to molten salts. Existing and proposed nuclear reactors vary widely in design, fuel type, coolant type, operating temperature, and neutron spectrum. As a result, the corrosion concerns for individual reactors vary significantly. This diversity in service environments poses a significant challenge for corrosion research because of the number of possible material-environment corrosion systems. The specific concerns for each reactor are discussed in more detail in Chapter 4.

Corrosion in reactors is a vast topic that depends on the specific reactor type and the exact material system within the reactor: it can occur in fuel systems and structural materials. Molten salt reactors generally operate in the range of 500–1000 °C and can include fueled salts (for fuel) and unfueled salts for coolant. The salts consist of fluoride or chloride salts that are frequently highly corrosive, although salt purity (i.e., concentration of contaminants such as water) can impact their degree of corrosiveness [22]. In the case of fueled salts, salt is also mixed with actinides and other fission products. Liquid metal fast reactors use sodium, lead, or lead-bismuth eutectic as the coolant. Sodium fast reactors operate in the range of 500–550 °C, and although sodium is generally considered compatible with structural metals, dissolution and mass transfer, as well as impurities in the sodium such as C, O, and N, are a concern. Lead- or lead-bismuth-cooled fast reactors operate in the range of 500–650 °C. Lead-based coolants are corrosive to structural metals and can lead to liquid metal embrittlement. Due to the high density of lead-based coolants, erosion corrosion is also a concern. High-temperature gas-cooled reactors operate at $>$ 700 °C and the major corrosion concern relates to impurities in the coolant gas, such as H_2, CH_4, N_2, O_2, H_2O, CO, and CO_2. Finally, water-based advanced reactors include water-cooled reactors operating with coolant temperatures $<$ 330 °C and have similar corrosion concerns as in the existing water-cooled commercial reactor fleet.

1.4 Conclusions

Characteristics of AM materials, including surface roughness, dislocation cells, porosity, and compositional heterogeneity raise concerns regarding their corrosion performance in advanced reactor environments. In-service evolution of AM microstructures, such as that caused by thermal exposure or irradiation damage, can complicate the situation even further by introducing new interaction mechanisms or affecting the existing interactions to a different extent. Given the enormous research areas that need to be covered, a down-selection in the corrosion systems focusing on specific AM materials for specific reactor applications is necessary to embrace AM technologies for advanced nuclear applications. Overall, there are major research needs to understand the similarities and differences in corrosion responses between AM and traditionally produced materials, and to identify the AM-specific corrosion issues in application-specific reactor environments.

2. OVERVIEW OF CORROSION MECHANISMS

Generally, corrosion in the context of structural alloys is the degradation of the metallic material by chemical or electrochemical reactions with the other species of the service environment. This is frequently an oxidation reaction with, for example, air or water. Corrosion leads to the conversion of the metal into another species such as an oxide compound or salt. This corrosion product may remain tightly adhered to the surface of the component being corroded; may occur within the bulk of the component; or may be removed from the surface of the component by spalling, for example. Corrosion becomes a concern when the engineering properties of the material are degraded or the geometry of the component are changed beyond acceptable engineering tolerances. Because corrosion processes are different for different materials and in different environments, corrosion issues are highly material-specific and environment-dependent. For a given alloy-environment combination, various factors can contribute to the corrosion process. While the alloy's composition and microstructure determine the general susceptibility of the material, the environment's corrosive species and pH level define the aggressiveness of the environment. The temperature at which the interactions take place between the material and its environment is perhaps the most important parameter since it determines the rate and extent of the corrosion process. Working together, all these parameters contribute to the corrosion behavior in a material-environment system.

Corrosion generally consists of electrochemical reactions that create anion and cation species from previously electrically neutral species. Metal atoms lose electrons to create cations in an oxidation half-reaction at the anode, while other species such as oxygen form compounds in a reduction half-reaction at the cathode. The flow of electrical charge is a necessary component to the corrosion reaction. The interference of this reaction by the presence of an adherent, protective film is called passivation. Corrosion can be classified by the appearance of the attack or the underlying mechanisms of the alloy-environment interactions. Table 1 shows the forms of corrosion commonly associated with engineering alloys.

2.1 Uniform Corrosion

The most common form of corrosion is uniform corrosion or general corrosion. Uniform corrosion refers to a form of corrosion in which the corroded areas occur evenly across the material surface in contact with its environment, resulting in a consistent loss of material thickness. Uniform corrosion appears as rust or tarnish on engineering alloys and can affect large amounts of materials because the attack occurs across the entire exposed surface. The metal reacts with oxygen, moisture, or other chemicals in its environment, losing electrons and combining with environmental elements to create corrosion scale. The corrosion scale may flake off or remain attached to the surface depending on the specific conditions. This corrosion scale can serve as a barrier, slowing down the corrosion rate by limiting the direct exposure of the metal to the environment. Uniform corrosion can affect additively manufactured (AM) materials

Table 1. Types of corrosion associated with engineering alloys.

Corrosion form	**Description**	**Causes**
Uniform corrosion	Gradual and even corrosion over the entire surface exposed to environment	Chemical and electrochemical reactions between metal and environment
Galvanic corrosion	Electrochemical process due to the coupling of dissimilar metals in electrolyte	Formation of an anode and a cathode
Crevice corrosion	Corrosion attack within narrow gaps where electrolyte is stagnant, limiting oxygen reduction, and causing differential aeration corrosion	Difference in oxygen concentration between the crevice and the outside environment
Intergranular corrosion	Corrosion attack along grain boundaries due to sensitization and depletion of protective elements	Loss of corrosion-resistant alloy elements near grain boundaries
Pitting corrosion	Localized corrosion attack in small pits or cavities, penetrating deep into the metal	Occurs in areas where protective oxide layer breaks down
Environmentally assisted cracking	Caused by combined action of stress and corrosive environment, classified by loading mode or cracking mechanisms	Interactions among material, environment, and stress
Dealloying	Preferential removal of one or more alloy elements	Different dissolution rates for different alloy elements

just as it affects traditionally manufactured materials. Several aspects of AM materials, such as microstructural variations, residual stresses, and surface roughness may particularly influence the general corrosion behavior of these materials.

While uniform corrosion may represent the greatest material loss in terms of quantity, it is not regarded as the most serious form of corrosion attack because it is relatively easy to evaluate and predict. Simple tests such as immersing samples in a fluid environment are often sufficient to evaluate the extent of uniform corrosion, and the results can be used for estimating the service lifetime of metal components. In contrast, most other forms of corrosion occur locally, and therefore the attack is limited to specific areas or parts. The occurrence of these forms of corrosion is more unpredictable and, therefore, is more likely to result in premature failures.

2.2 Localized Corrosion

Localized corrosion occurs when a small region is more susceptible to corrosion than its surroundings. Localized corrosion can include pitting, crevice, and intergranular corrosion morphologies, and frequently involves the galvanic corrosion mechanism. Localized corrosion is the larger concern for component failure because of its ability to cause rapid and unexpected failure. Localized corrosion can occur rapidly and cause hidden damage that is difficult to detect.

2.2.1 Galvanic corrosion

Galvanic corrosion, also known as bimetallic corrosion, is an electrochemical process that involves two dissimilar metals and is driven by the potential difference between them. When the two metals are electrically connected and immersed in an electrolyte, a galvanic cell is created, forming an electrical circuit and resulting in the preferential corrosion of one material (the anode) and the suppression of attack (also termed “protection”) of the other material (the cathode).

Galvanic corrosion is largely controlled by the potential difference between the electrodes, which refers to their tendency to lose or gain electrons. This can be affected by several factors, including relative positions of two alloys in the galvanic series [23], the environment, passivity, and geometric considerations. The galvanic series refers to the relative potential of different electrode materials in an electrolyte with respect to a standard electrode. A passivation layer on an electrode results in a change of the position of the material in the galvanic series, leading to a different galvanic effect. In addition, distance from the electrode junction affects galvanic corrosion due to the resistance of the electrolyte. Galvanic corrosion can become very localized in a high-resistance environment because the current density will decline sharply in a low-conductivity electrolyte when moving away from the junction of two alloys. Similarly, the difference in the surface areas of the anode and cathode can exert a strong impact on galvanic corrosion due to the current densities achievable. A large ratio of cathodic to anodic surface areas would increase the current density at the anodic area considerably, leading to a greater corrosion rate. Galvanic corrosion would be expected in AM materials, especially when different AM materials with different compositions are used together in corrosive environments. A galvanic couple may be formed between different AM parts or even within one AM component between different areas exhibiting compositional heterogeneity.

2.2.2 Crevice corrosion

Crevice corrosion is a localized form of corrosion that occurs in narrow gaps or crevices between surfaces. Any area with a small gap between two surfaces, such as the mating surfaces of components or cracks within components, can generate favorable conditions for crevice corrosion in a fluid environment. The gap between surfaces must be wide enough to permit liquid to enter but also be narrow enough to restrict convection for crevice corrosion to occur. The driving force of this form of corrosion is a concentration cell formed between the electrolyte within the crevice and outside the crevice. Inside the crevice, oxygen becomes depleted because of the stagnant condition. Consequently, oxygen reduction stops in this area while metal dissolution continues, leading to variations of pH and ion concentration in the crevice and creating a microelectrochemical cell between the crevice area (anode) and the external surface (cathode). Thus, the crevice area experiences accelerated corrosion while the open surface benefits from cathodic protection.

Crevice corrosion poses a concern for AM materials, much as it does for traditionally manufactured materials. Certain attributes of AM components, such as complex geometries, may generate a condition vulnerable to crevice corrosion. This could be a concern for components with small features, such as those fabricated by laser powder bed fusion. Crevice corrosion may also be a concern for net-shape components with high surface roughness, such as those fabricated via wire directed energy deposition. Although the surface roughness is on a smaller scale in laser powder bed fusion, the unique geometry of laser powder bed fusion (LPBF) surface roughness may also make the component vulnerable to crevice corrosion. Understanding the crevice corrosion mechanism and how an AM component would interact with its environment is critical for using AM in real-world applications.

2.2.3 Pitting corrosion

Pitting corrosion is an extremely localized and highly destructive form of corrosion that occurs on metal surfaces. The main trait of pitting corrosion is the formation of small pits or cavities. Pitting corrosion typically results when a passive film on a surface is damaged or disrupted, allowing the creation of a galvanic cell. As the pit forms, the local environment within the pit will generally become even more conducive to continued corrosion, accelerating pit formation and penetration into the material. Pitting corrosion is of particular engineering concern because it is frequently hard to detect; for example, a small (microns to millimeter) pinhole on the surface of the metal can hide a large hole within the material. The extent of pitting damage is also difficult to measure and compare quantitatively because of the varying depths and numbers of pits that may occur under identical conditions. These difficulties in detection and evaluation make pitting one of the most insidious forms of corrosion that may lead to severe structural issues or even catastrophic failures.

Pitting corrosion begins with the breakdown of the protective passive film on a metal surface due to local defects, impurities, or aggressive substances. Once the passive film is compromised at these locations, metal dissolution occurs in the presence of an electrolyte, making them anodic sites. The surrounding areas, however, become cathodic sites where oxygen reduction takes place. This separation of anodic and cathodic sites creates a localized electrochemical cell, and the anodic sites become the focus point of intense electrochemical reactions. Pitting corrosion usually requires a long incubation period to initiate. Once started, a pit can penetrate deeply into the metal in a self-stimulating and self-propagating manner. The rapid dissolution of metal within the pit produces excessive metal ions in the area, resulting in an increased concentration of corrosive agents and acidity and therefore enhances the localized corrosion. This positive feedback makes pitting an autocatalytic corrosion process.

Pitting could be a significant factor for AM materials. Inhomogeneous composition and microstructure, surface roughness, and residual stress can all influence the local passivation condition, generating a condition vulnerable to pitting attacks. Understanding the interactions between AM materials' unique characteristics and the mechanism of pitting corrosion is crucial for effectively managing this form of corrosion attack.

2.2.4 Intergranular corrosion

As the name suggests, intergranular corrosion is another form of localized corrosion that preferentially attacks grain boundaries. Compared to the grain interiors, grain boundaries are more reactive because of their high defect density and segregation of impurities and alloying elements. Due to the higher energy state of grain boundaries, corrosive agents can attack grain boundaries more readily than the bulk material. In addition, intergranular corrosion frequently results from the localized loss of elements that form passivating films at grain boundaries. These elements may migrate away from the grain boundary into the bulk of the grain due to radiation-induced segregation, be selectively leached into the electrolyte, or become locally bound in an insoluble, non-film-forming precipitate. As a result, a localized galvanic couple forms, with the grain boundary being anodic and the surrounding passivated grains being cathodic, causing preferential corrosion of the grain boundary.

One example of this preferential attack on grain boundaries is the intergranular corrosion on sensitized stainless steels (SS). When heated to temperatures above 500 °C, chromium carbide ($Cr_{23}C_6$) precipitates, removing Cr from the solid solution. This precipitation process tends to occur along grain boundaries where microstructural inhomogeneities are more frequent. As a result, the Cr concentration on and near the grain boundaries is depleted, degrading the passivation layer. At the sensitization temperature, C diffuses much faster than Cr toward grain boundaries, providing abundant C for precipitation, exacerbating the Cr depletion. Chromium content can be reduced locally to very low levels, leaving grain boundaries unprotected. This localized corrosion mechanism makes materials vulnerable to forming cracks and voids along grain boundaries, further accelerating the corrosion process.

Intergranular corrosion could be a concern for AM materials. Manufactured layer-by-layer, AM materials have unique boundary structures. These boundaries may be vulnerable to intergranular attack, especially due to additional elemental segregation that results from the printing process. Also, AM materials may experience thermal cycles during or after printing that resemble sensitization. These factors can potentially influence the passivation condition around grain boundaries, making them vulnerable to corrosion attack.

2.2.5 Environmentally assisted cracking

The environmentally assisted cracking (EAC) phenomenon is a specific form of corrosion involving internal or external stresses. It is difficult to detect and predict, and therefore is a serious concern for unexpected and sudden failures. Unlike other forms of corrosion, EAC is not defined solely by the corrosion system comprising the vulnerable material and the corrosive environment. Instead, the interaction between the corrosion system and mechanical stresses is essential. The synergistic effect of the corrosion environment and mechanical stresses is crucial for EAC because it can provide positive feedback for the extension of cracks.

There are several forms of EAC, each characterized by specific cracking mechanisms and loading conditions. Corrosion fatigue is a form of degradation caused by cyclic stresses within a corrosive environment. Fatigue damage resulting from cyclic stresses can be exacerbated by the corrosive environment. Conversely, stress corrosion cracking (SCC) can arise if the stress (especially tensile stress) is static and no significant fatigue damage occurs. The interaction between the corrosive environment and stress can cause or accelerate crack propagation. Various forms of SCC can be categorized either by their cracking path (e.g., intergranular SCC), or by their cracking mechanisms (e.g., chloride SCC). Furthermore, when hydrogen is present, EAC can also manifest itself as hydrogen embrittlement. Hydrogen generated by corrosion can penetrate into the material structure, weakening its mechanical properties and interacting with the stress field around the crack. If a liquid metal, such as sodium or lead, is the corrosive environment, the interactions between the liquid metal and susceptible material can also degrade the material's cracking resistance. This form of attack primarily focuses on grain boundaries or other metallurgical features, leading to liquid-metal embrittlement.

Despite a wide range of cracking phenomena, all forms of EAC require the synergistic actions of material, environment, and stress. A combination of an aggressive environment and a vulnerable material alone is not sufficient for EAC; the interactions between stress and environment are essential for EAC to occur. For AM materials, the consideration of EAC is not different from that of traditionally produced alloys. The main characteristics of AM materials such as porosity, inhomogeneous composition, active boundaries, and internal stress can all contribute to the development of EAC.

2.2.6 Dealloying

Dealloying is a specific form of corrosion that involves the preferential removal of one or more elements from an alloy, leaving behind a porous or spongy microstructure with altered composition. Selective dealloying occurs locally and affects specific areas of the alloy. Selective dealloying occurs because one element is more susceptible to corrosion or to dissolution in a specific environment compared to the others. The more corrosion-resistant component(s) may remain relatively unaffected while the more susceptible component(s) are removed from the alloy. The most famous example of dealloying is the "dezincification" of brass, in which zinc is preferentially corroded, resulting in a porous, copper-rich surface. In general, selective dealloying is a distinct form of corrosion characterized by the preferential removal of elements from an alloy, leading to a change in its composition and structure.

Dealloying can affect AM materials if favorable conditions emerge. AM microstructure resulting from layer-by-layer printing may corrode preferentially for certain components, exacerbating the extent of local dealloying. The inhomogeneous composition of AM materials may enhance preferential corrosion. Understanding the potential for dealloying and its effects on AM materials is crucial for ensuring their reliable performance in real-world applications.

2.3 Additional Corrosion Phenomena

Liquid metal corrosion can result from exposure to sodium, lead, or other liquid metals, and can cause leaching, loss of material, formation of new compounds, cracking, and embrittlement. Often, the loss of the oxide layer of the material is a driver of liquid metal corrosion. Control of impurity content is important for reducing liquid metal attack, as is control of the number and type of materials systems in contact with the liquid metal. Carburization and decarburization are a concern for steels and are affected by the activity of carbon in each component in the material-liquid metal system. Mass loss can also be affected by the amount of oxygen dissolved in the liquid metal, as it affects the stability of the oxide film on the structural alloy.

Corrosion from high-temperature helium can also occur and is generally due to the presence of impurities in the gas, such as O, N, H_2O, H, CO, or CO_2. Carburization, decarburization and oxidation are all concerns for structural materials and are controlled by the partial pressures of the impurities in the gas.

Erosion-corrosion and flow-assisted corrosion result from the continuous removal of a normally adherent corrosion layer by fast-flowing fluid, resulting in ongoing corrosion processes. The poorly soluble corrosion product is dissolved due to high flow rates of unsaturated fluid, allowing dissolution and exposure of the metal beneath. Flow-assisted corrosion is not the same as erosion (which results from mechanical means such as particulate or bubble impingement against the surface), though the result is generally similar. A key aspect of flow-assisted corrosion is its dependency on fluid flow rate. Since this form of corrosion depends on the removal or weakening of the protective layer to facilitate ongoing corrosion, flow velocity becomes a critical factor, alongside temperature, environmental chemistry, and material microstructure.

2.4 Synergy with other Degradation Modes

Corrosion can interact with various other factors and mechanisms in complex ways, leading to synergistic effects that accelerate material degradation and structural failure. Irradiation can interplay with corrosion in two ways, discussed in further detail in Section 4.6. Ionizing radiation can create free radicals in the coolant, leading to increased chemical reactivity and possibly enhancing corrosion. Irradiation can also induce microstructural changes in the material that may make it more susceptible to corrosion. The former effect is transient and requires ongoing irradiation to test, while the latter is a persistent effect outside of a radiation field. Corrosion can also interact with creep and fatigue. When the two are combined, the damage induced by corrosion can accelerate the deformation caused during creep, fatigue, and creep-fatigue. In addition, fretting can remove protective layers that prevent corrosion by mechanical wear, accelerating material loss and damage. Finally, thermal aging can lead to changes in microstructures (such as precipitation of phases) that may make the material more susceptible to corrosion, e.g., either by reducing protective elements in solution or by forming precipitates that disrupt protective films.

2.5 Review of Corrosion of Austenitic Stainless Steels

Corrosion protection of stainless steel is based on the formation of a thin, passive film composed primarily of chromium oxide that protects the underlying material from corrosive attack. Depending on the specific grade of stainless steel, other elements such as Ni, Mn, Mo, W, and Cu have been added to improve corrosion resistance in different environments and to stabilize the fcc austenite phase. Although stainless steels are generally highly resistant to corrosion in many environments, corrosion may still occur. In general, corrosion begins with disruption of the chromium oxide film, which may result from outside mechanical forces, such as scratching, or by localized stresses resulting in dislocations intersecting the surface. Grain boundaries can also allow secondary phases to precipitate on the surface, disrupting the film.

Once the passive film has been broken, localized corrosion can begin. Ions in the surrounding medium allow for anodic reactions to corrode away unprotected regions of the steel. This is readily seen in pitting and crevice corrosion. Localized corrosion can also occur along grain boundaries. In austenitic stainless steels, precipitation of chromium carbides near grain boundaries results in localized depletion of the Cr concentration at the grain boundary, reduces the passivation at the grain boundary, and allows for intergranular attack.

The effectiveness of the passivation layer is also reduced by the presence of hydrogen. High concentrations of hydrogen can cause the structure and composition of the passivation layer to change. The presence of hydrogen also changes the electrochemical environment of the film and the base metal, reducing the stability of the passivation layer, heightening oxidation and dissolution kinetics, and promoting pitting and intergranular corrosion.

2.6 Review of Corrosion Studies on Additively Manufactured Metals in Nuclear and Non-Nuclear Industries

As additive manufacturing has increased in engineering feasibility, corrosion testing of AM materials has followed. However, the variety of AM techniques and the complexity of AM microstructures that can result in a given composition of material (e.g., 316 stainless steel) mean that a clear picture has yet to emerge on the exact interplay of manufacturing parameters (resulting in microstructure) and the corrosion behavior. Below is a summary of a brief selection of the literature which provides a high-level view of corrosion observations on AM austenitic stainless steels. Many of the references cited here contain further summaries within and will be discussed in more detail in Chapter 5.

Some studies indicate that the corrosion resistance of AM stainless steels has improved over their conventionally wrought counterparts in water and sodium chloride environments [24] despite the complexity of the interplay between microstructure and corrosion mechanisms, and provided that the material does not contain significant porosity. The mechanism for this improvement is not determined to date, but it is hypothesized to be a result of improved chromium oxide film thickness. This improved thickness is thought to arise from the high density of cellular dislocation walls with chemical segregation that could promote the growth of a denser and more stable passive film [24]. However, this mechanism would clearly be subject to the type and degree of chemical segregation at the cellular dislocation walls, which is likely controlled by process parameters.

Several general trends start to become clear from the literature concerning the presence of pores, δ-ferrite, and cellular dislocation structure. Some evidence indicates that increasing both the porosity and the pore size increases the stress corrosion cracking (SCC) growth rate [10]. There is also evidence that increasing porosity decreases the breakdown voltage of stainless steels [25], possibly because the pores can serve as nucleation sites for crevice or pitting corrosion. In addition, the presence of δ-ferrite may alter the corrosion of AM 316, likely due to its impact on the formation of the chromium oxide passive film. The presence of δ-ferrite within powder DED-fabricated 316L SS affected its irradiation-assisted stress corrosion cracking (IASCC) behavior with respect to that observed in wrought material. Cracks propagated along the δ-ferrite/γ-austenite phase boundaries, likely due to the reduction in grain boundary sliding and dislocation interactions at boundaries providing nucleation sites for cracks [26]. Anisotropy of the δ-ferrite distribution in 316L fabricated by wire arc additive manufacturing also affects pitting and uniform corrosion rates, with less phase volume and more finely dispersed δ-ferrite, improving the general corrosion rate [27]. The σ phase is also detrimental and has been reported to increase pitting corrosion [28]. Heat treatment generally improves corrosion behavior [29], likely due to the dissolution of deleterious phases.

Very little work has been published on the effect of surface roughness on corrosion of AM 316 material. Although surface roughness is known to impact corrosion properties [30], most AM corrosion studies have taken place on milled and polished samples [30]. Several studies examined the effect of surface modifications on corrosion behavior (e.g., sandblasting) and build surface orientation on corrosion. Mixed results arose for surface modifications intended to smooth the part, with some improving corrosion behavior and some making it worse [30]. Build surface orientation had a clearer impact, although other factors impacting the microstructure, rather than just the surface roughness, could be responsible [30].

In addition, very little work has been published regarding the corrosion of AM components for nuclear applications to date and the focus has been on water environments [10, 26, 31, 32]. Stress corrosion cracking in AM 316 followed the build direction of stress-relieved 316L SS built by laser powder bed fusion, while recrystallized material had a similar SCC growth rate as wrought material [10]. However, the information about AM corrosion in water and sodium chloride environments should be transferable (within limits) to the corrosion behavior of AM materials for nuclear applications, especially within other corrosive environments such as liquid metals, molten salts, and high-temperature helium provided a mechanistic understanding of corrosion and microstructure is applied.

2.7 Summary and Conclusions

This chapter provides a summary of corrosion modes that are commonly observed in metals, with a focus on 316 stainless steel. General and localized corrosion mechanisms are discussed that can occur in a variety of environments, including water, liquid metal, molten salts, and high-temperature helium. The corrosion behavior of 316 SS is largely controlled by the presence and characteristics of the passivating chromium oxide film, with better corrosion resistance coming from thick, unbroken films. The film can be broken by wear or by the presence of second phases, making the material vulnerable to pitting corrosion.

The literature on corrosion of AM materials is largely focused on water and sodium chloride-based environments and very few nuclear-specific corrosion studies have been performed. In general, the corrosion behavior of AM materials is more complex than that of wrought materials due to the more complex surfaces and microstructures. However, some evidence indicates that the corrosion resistance of AM materials with low porosity may be better than wrought material, although the mechanism is currently unexplained. The presence of porosity increases corrosion, while the effect of the presence of the δ-ferrite phase remains uncertain. Those nuclear-specific studies also focus on water environments and largely study SCC or IASCC. The effect of surface roughness on corrosion behavior has not been systematically studied.

3. ENGINEERING CONCERNS FOR CORROSION BEHAVIOR

Corrosion presents multiple engineering concerns in the context of nuclear reactors. Some specific concerns for nuclear reactor corrosion include corrosion of the reactor pressure vessel (or any vessel in any advanced reactor design) and associated structures, corrosion of the material facing the fuel, such as fuel cladding or pins containing fueled salt, and corrosion of the cooling systems, including primary and secondary loops. In terms of these concerns, first and foremost, corrosion can impact structural integrity of components, serving as a failure mechanism that can limit lifetimes. In addition, general corrosion can release corrosion products that deposit on other parts of the plant, reducing heat transfer ability or impacting a component's mechanical ability. Thus, corrosion adds to maintenance costs to measure, prevent, and mitigate corrosion in service. As a result, materials must be selected carefully not just for their desired service properties (e.g., mechanical strength), but also for their compatibility with the service environment (e.g., to avoid pitting corrosion) and each other (e.g., to avoid galvanic corrosion).

3.1 Component Failure Mechanisms

In an engineering context, corrosion causes component failure by several major mechanisms, including loss of load-bearing capacity, embrittlement, leakage, and degradation and loss of functionality of other components. Loss of load-bearing capacity is arguably the most likely cause of component failure in a nuclear power plant. It can occur due to a relatively uniform loss of load-bearing material, such as uniform corrosion on light-water reactor (LWR) fuel cladding, the reduction of cross-sectional area, or by the formation of cracks or pits through the material. Loss of load-bearing capacity limits the lifetime of a component due to inability to sustain the designed mechanical stresses. Embrittlement can lead to catastrophic failure of a component; some degree of ductility is designed for component failure via deformation without sudden, complete fracture. Leakage can be caused by mechanisms such as cracking or pitting, and leads to the infiltration of one contained environment into another environment (e.g., coolant infiltration past a pump seal). Degradation and loss of functionality may occur when corrosion products build up; for example, freezing a valve or clogging a heat exchanger.

3.2 Corrosion Codes and Standards

Evaluation of material corrosion is standardized in a series of ASTM procedures (ASTM International was formerly known as the American Society for Testing and Materials). Below is a discussion of several important ASTM standards for corrosion testing; however, the ASTM standards are extensive and detailed to cover many different materials and types of corrosion and corrosion testing. It is important to search for relevant ASTM standards before conducting any new type of corrosion test. ASTM G1, “Standard Practice for Preparing, Cleaning, and Evaluating Corrosion Test Specimens,” specifies the proper practices for preparing, cleaning, and evaluating corrosion specimens. ASTM G31, “Standard Guide for Laboratory Immersion Corrosion Testing of Metals," provides guidance for immersion testing. Although ASTM G31 discusses static testing, ASTM G31/A (an Annex to ASTM G31) provides a discussion for dynamic corrosion testing under flowing conditions. Procedures for testing intergranular corrosion of stainless steels are primarily described in ASTM A262, "Standard Practices for Detecting Susceptibility to Intergranular Attack in Austenitic Stainless Steels" and ASTM A763, "Standard Practices for Detecting Susceptibility to Intergranular Attack in Ferritic Stainless Steels." However, for nickel-rich alloys containing chromium, ASTM G28, "Standard Test Methods for Detecting Susceptibility to Intergranular Corrosion in Wrought, Nickel-Rich, Chromium-Bearing Alloys," is applicable. ASTM G71, "Standard Guide for Conducting and Evaluating Galvanic Corrosion Tests in Electrolytes," offers guidance for assessing the compatibility of dissimilar metals when in contact with each other in an electrolyte (galvanic corrosion).

Test methods for analyzing pitting corrosion in stainless steels are described in ASTM G48, "Standard Test Methods for Pitting and Crevice Corrosion Resistance of Stainless Steels and Related Alloys by Use of Ferric Chloride Solution." Analysis of the results of pitting corrosion testing is governed by ASTM G46, "Standard Guide for Examination and Evaluation of Pitting Corrosion." An alternative method of investigating pitting in stainless steel is to measure the pitting potential electrochemically. The procedure for doing this is outlined in ASTM G150, "Standard Test Method for Electrochemical Critical Pitting Temperature Testing of Stainless Steels and Related Alloys." The mechanisms behind pitting and crevice corrosion are similar, so the testing procedures are similar and the same ASTM standards can be applied. ASTM G150 includes discussion of dynamic testing, which may involve flow conditions.

Stress corrosion cracking is a significant issue in steels, particularly in austenitic stainless steels. Stress corrosion cracking is a phenomenon that occurs in a material under stress. Understanding the stress corrosion cracking behavior of a material is important for predicting its long-term performance. Investigation of stress corrosion cracking in steels is complex and governed by many different standards. The testing required depends on the material and the environment. When investigating a new material, ASTM G129, "Standard Practice for Slow Strain Rate Testing to Evaluate the Susceptibility of Metallic Materials to Environmentally Assisted Cracking," is a good place to start because it evaluates how susceptible the material is to environmentally assisted cracking (EAC).

An alternative to standard submersion corrosion testing is electrochemical corrosion testing. ASTM G5, "Standard Reference Test Method for Making Potentiodynamic Anodic Polarization Measurements," covers potentiodynamic anodic polarization measurements, while ASTM G59, "Standard Test Method for Conducting Potentiodynamic Polarization Resistance Measurements," covers potentiodynamic polarization resistance measurements. A more material-specific test standard is ASTM G61 "Standard Test Method for Conducting Cyclic Potentiodynamic Polarization Measurements for Localized Corrosion Susceptibility of Iron-, Nickel-, or Cobalt-Based Alloys," which applies to potentiodynamic polarization measurements for Fe-, Ni-, and Co-based alloys. ASTM G3, "Standard Practice for Conventions Applicable to Electrochemical

Measurements in Corrosion Testing," sets the standard for representing the results of the electrochemical corrosion data, while ASTM G102, "Standard Practice for Calculation of Corrosion Rates and Related Information from Electrochemical Measurements," standardizes the methods for calculating corrosion rates and other information from the electrochemical tests, while ASTM G82, "Standard Guide for Development and Use of a Galvanic Series for Predicting Galvanic Corrosion Performance," describes how to develop and use a galvanic series to rank materials in a particular corrosion system for their likelihood of galvanic corrosion.

Several areas of corrosion testing relevant for advanced reactors do not have many or any ASTM standards, such as high-temperature helium testing or specific standards for testing additively manufactured (AM) material. ASTM G111, "Standard Guide for Corrosion Tests in High Temperature or High Pressure Environment, or Both," may be relevant for high-temperature helium or liquid metal resting. ASTM G32, "Standard Test Method for Cavitation Erosion Using Vibratory Apparatus," may be relevant for evaluating cavitation corrosion in liquid metals.

Testing procedures for corrosion are widely covered by ASTM. Conversely, American Society of Mechanical Engineers (ASME) Section III (which covers advanced reactors) does not generally discuss corrosion and its effect on mechanical performance. However, ASME Section XI, "Rules for Inservice Inspection of Nuclear Power Plant Components," provides guidelines for inspection, testing, and maintenance of nuclear power plants, including assessing the impact of corrosion on structural integrity. Nonetheless, ASME Section XI focuses on LWR technology currently. Rules and standards relevant to advanced reactors are under development. In addition, no specific ASTM standards have been written for corrosion testing of materials produced through additive manufacturing.

3.3 Qualification and Regulation

The U.S. Nuclear Regulatory Commission (NRC) considers corrosion a significant factor in ensuring the safe and reliable operation of nuclear power plants. Although an extensive discussion of the NRC considerations of corrosion is beyond the scope of this report and the Advanced Materials Manufacturing Technologies (AMMT) program in general, the NRC's regulatory framework includes various requirements, guidelines, and inspections aimed at preventing, monitoring, and managing corrosion-related issues in nuclear facilities. The NRC establishes and enforces regulations and standards to ensure the safe operation of nuclear power plants. These regulations cover various aspects of plant design, construction, and operation, including corrosion prevention and control. When nuclear power plants apply for licensing or license renewal, licence applicants must demonstrate how they will manage aging effects, including corrosion, during operation. Different components of the plants are subjected to different temperatures, pressures, flows, radiation fluxes, and chemical environments. For a material to be qualified for use in a particular application, the environment needs to be defined and testing must show that the material can reliably perform in that environment. The NRC also requires nuclear power plant operators to select materials for critical components (such as reactor pressure vessels, piping, and containment structures) that are resistant to corrosion under the expected operating conditions. Materials are chosen to minimize the risk of corrosion-related failures. Beyond initial selection of material, the NRC mandates several monitoring systems, including environmental monitoring and in-service inspection. Environmental monitoring programs assess the quality of cooling water, reactor coolant, and other fluids that come into contact with reactor components and include testing for impurities and chemical parameters that could accelerate corrosion. In-service inspection is required for critical components, including piping, pressure vessels, and reactor internals, to detect corrosion and other forms of degradation. These inspections are performed in accordance with ASME Section XI and other applicable codes and standards. In addition, the NRC denotes corrosion allowances in absolute loss of thickness (e.g., 50 μm) and acceptable corrosion rates (e.g., 0.76 μm/year) for license applications [33].

The U.S. NRC oversees the licensing of nuclear power plants and reviews the proposed design. As part of their review, they consider the materials proposed for each application and determine whether the material has been sufficiently demonstrated to perform in such a manner that it can be reasonably ensured that all integrity criteria are met. Therefore, the developer or applicant needs to develop and compile an environmental effects evaluation through demonstration for regulatory approval.

Testing to ASTM standards is important for qualifying material for use in reactors. For in-reactor material, intergranular corrosion tends to be a significant issue. ASTM A262, “Standard Practices for Detecting Susceptibility to Intergranular Attack in Austenitic Stainless Steels,” is a standard test used to measure the degree of sensitization in reactor materials. That standard couples with ASTM G108, “Standard Test Method for Electrochemical Reactivation (EPR) for Detecting Sensitization of AISI Type 304 and 304L Stainless Steels,” which describes the method of performing electrochemical potentiokinetic reactivation tests. This coupling provides a more quantitative method for measuring the degree of sensitization, though the test is written specifically for 304 and 304L stainless steel.

The results of testing are used as part of the design basis for the licensing of nuclear power plants. The reactor designer needs to show that the material will be able to perform safely and reliably in its intended application. The design basis for nuclear power plants is given in Title 10 of the Code of Federal Regulations Part 50 (10 CFR Part 50), Appendix A: General Design Criteria for Nuclear Power Plants: Criterion 1—Quality Standards and Records. The full relevant text is reproduced below.

> “Structures, systems, and components important to safety shall be designed, fabricated, erected, and tested to quality standards commensurate with the importance of the safety functions to be performed. Where generally recognized codes and standards are used, they shall be identified and evaluated to determine their applicability, adequacy, and sufficiency and shall be supplemented or modified as necessary to assure a quality product in keeping with the required safety function. A quality assurance program shall be established and implemented to provide adequate

> assurance that these structures, systems, and components will satisfactorily perform their safety functions. Appropriate records of the design, fabrication, erection, and testing of structures, systems, and components important to safety shall be maintained by or under the control of the nuclear power unit licensee throughout the life of the unit."

3.4 Summary and Conclusions

Corrosion-induced failure and degradation are major engineering concerns for nuclear power plants. Accordingly, a large array of regulations surrounds corrosion testing and in-reactor assessment. ASTM standards discuss testing methodologies for many different kinds of corrosion and materials. Before any corrosion tests are performed within the AMMT program, a search should be performed to determine if a relevant ASTM standard exists. However, not all corrosion tests that could be envisioned for advanced reactor material-environment systems have ASTM standards. In addition, no ASTM standard exists that is specific for testing AM materials. If a relevant standard does not exist, the program should develop an internal standardized methodology for testing and consider promoting new ASTM standards. While ASTM standards focus on material testing, ASME standards in Section XI focus on surveillance of corrosion in a nuclear plant itself. However, Section XI is largely focused on LWRs. The applicability of Section XI standards for advanced reactors must be assessed. Furthermore, corrosion of advanced reactors and AM materials must be considered with respect to the concerns of the NRC and may be another topic of collaboration between AMMT and the office of regulatory research within the NRC. Although corrosion allowances are discussed in NRC regulations, these may need to be re-assessed for AM materials.

4. REACTOR-SPECIFIC CORROSION ISSUES

Because of the differences in coolant and/or moderator (for thermal-spectrum reactors), each reactor type has its own primary corrosion issues. Table 2 shows the typical service environment and structural materials for different reactor types. As expected, different service environments result in different corrosion responses even if the same alloy is employed. Consequently, corrosion issues in nuclear applications are always reactor-specific and can only be evaluated by understanding the specific alloy-environment system. While a wide range of construction materials may be used in reactor construction, the major structural materials in the current reactors and future advanced reactors are nickel alloys and iron-based stainless steels.

Table 2. Service environment and structural materials of different reactor types.

Reactor Type	**Environment**			**Materials**
	Coolant	**Moderator**	**Temperature**	
LWR	Water	Water	290 - 320 °C	SS, LAS, Ni alloys
MSR	Fluoride or chloride salt	Graphite, Zirconium hydride	600 - 750 °C	Ni alloys, SS
SFR	Sodium	-	500 - 550 °C	SS, F/M, Ni alloys
LFR	Lead, lead-bismuth	-	480 - 650 °C	F/M, ODS, SS, Ni alloys
HTGR	Helium	Graphite	750 - 950 °C	Graphite, SiC, Ni alloys, refractory metals

4.1 Light Water Reactors

For light water reactors (LWRs), light water is used as both the coolant and the moderator. LWRs operate at temperatures around 290–320 °C with pressures in the range of 1000–2200 psi (6.9–15.2 MPa). The structural materials in contact with water are mostly low-alloy steels (LAS), austenitic stainless steels (SSs), and Ni-based alloys. As a result, the main corrosion issues concerning LWRs are high-temperature aqueous corrosion for LAS, SS, and Ni-alloys.

A combination of high-temperature water and mechanical stress creates a favorable condition for a stress corrosion cracking (SCC) attack. In fact, SCC has been the leading degradation mechanism for SS and nickel-based alloys in LWRs since the 1980s [34]. Significant progress has been made for SCC mitigation based on decades of research and operational experience. Today, the water chemistry and purity is strictly controlled to eliminate corrosive species and to lower the corrosion potential [35]. Special attention has been paid to welds where sensitization can take place due to the thermal cycles experienced by the welds [36]. Post-production heat treatment is also required to lower the detrimental effects of residual stress.

In the reactor core regions of LWRs, irradiation can not only deteriorate the material's microstructure with displacement damage, but also increase the reactive species in water with radiolysis. This condition leads to irradiation-assisted SCC (IASCC), a more severe form of SCC. IASCC has been a difficult issue for LWRs because many variables can contribute to its occurrence simultaneously. While irradiation defects and radiation-induced segregation of chromium and other elements alter the material's microstructure, highly localized deformation modes also make irradiated materials more susceptible to SCC attack [37]. Despite decades of effort, a comprehensive understanding of the factors controlling IASCC has not emerged. As LWRs age, IASCC may become a critical issue. Furthermore, irradiation can contribute to general corrosion as well. Radiolysis may influence the corrosion environment, leading to higher corrosion rate.

Cracking of Alloy 600 (and Alloy 182) was a widespread issue for Ni-based alloys until it was replaced with Alloy 690 in recent years. Alloy 600 is vulnerable to SCC, and water chemistry control is not effective in lowering its cracking susceptibility [38]. The severity of cracking peaks around the Ni-NiO interface, and the Cr content of Alloy 600 (16 wt%) seems insufficient to protect it from grain-boundary oxidation. Alloy 690, however, has a Cr concentration almost twice as great (29 wt%) as that of Alloy 600, preventing SCC.

In addition, flow-accelerated corrosion can affect the secondary side of steam generators in LWRs and can compromise their structural integrity [39]. With flow acceleration, corrosion can take place when the protective layer on the pipes and equipment is eroded due to the mechanical effect of flow, leading to wall thinning or failures.

4.2 Molten Salt Reactors

Molten salt reactors (MSRs) use liquid salts either as a coolant to remove fission heat from the fuel (unfueled salt), to entrain the fuel itself (fueled salt), or possibly both. The salts can be either fluoride or chloride salts [22]. A mixture of salts is often selected to reduce their melting point, providing a wider temperature range before boiling. Unfueled fluoride salt compositions include $LiF-BeF_2$ (FLiBe), LiF-NaF-KF (FLiNaK), $KF-ZrF_4$, and unfueled chloride salts compositions include NaCl-KCl, $KCl-MgCl_2$, and $NaCl-KCl-MgCl_2$ [40]. Depending on the design, MSRs can have either a thermal or fast neutron spectrum. Small quantities of other salts may be added to control the redox potential of the salt system, which is a fundamental mechanism to control the corrosion behavior. For thermal MSRs, graphite or zirconium hydride are used as a moderator. The nuclear fuel used in MSRs can be dissolved in molten salts, or in a solid form such as TRISO (TRi-structural ISOtropic) particles. MSRs are typically operated at 600–750 °C and the materials used are mostly nickel-based alloys such as Hastelloy N. Among many advantages of MSRs, excellent thermal properties and a wide operating temperature window at near atmospheric pressure are the main benefits of using molten salts as a heat transfer medium.

Molten salts are highly corrosive for most structural materials. Generally, any oxide film on the surface of an alloy will be removed when in contact with molten salts, negating the ability to manage corrosion through a passivation strategy. The selective leaching of a material's constituents is the main corrosion process, making the formation energies of various salt compounds the key factors of molten salt corrosion. Among the major alloying elements in structural steels (i.e., Fe, Ni, and Cr), Cr is the most susceptible constituent to be dissolved in fluoride salts, and Ni is the least susceptible constituent [22]. For this reason, alloys with high Cr concentration tend to perform worse, and Ni-based alloys are the preferred choice in molten salt environments.

To mitigate the corrosion attack of structural materials, redox potential control can be employed. By introducing a reducing agent such as H_2, Be, or UF_3 and EuF_2 into the system, the redox potential can be reduced and therefore lower the susceptibility to corrosion in molten salts [41]. Impurities in molten salts such as moisture or tritium (from transmutation) can affect the redox potential. In addition, in fueled salts, the fission product Te can react with Cr to form a brittle phase along grain boundaries, leading to intergranular cracking. This Te-induced embrittlement is attributed to the preferential diffusion of Te along the grain boundaries.

For a molten salt system containing different structural materials, the local potential difference can drive the transfer of cations. Chromium removed from a steel component can deposit on a graphite component in a molten salt system. Similarly, if the system is not isothermal, mass transfer can occur along a temperature gradient. While material dissolution occurs at the hot location, material can deposit at cold sites due to decreased solute solubility.

4.3 Liquid Metal-Cooled Reactors

4.3.1 Sodium-cooled fast reactors

A sodium-cooled fast reactor (SFR) is an advanced reactor design that utilizes liquid sodium as a coolant. With a typical operating temperature of 500–550 °C, liquid sodium is an excellent heat transfer medium. Sodium has low vapor pressure, high thermal conductivity and heat capacity, and a large liquid-temperature range below boiling (from 98 to 883 °C). These thermal properties allow SFRs to be operated at near atmospheric pressure and to have a high-power density with a low coolant volume fraction [42]. While using liquid sodium as a coolant has significant advantages, it does pose some technical challenges. Liquid sodium violently reacts with oxygen in air, creating a danger if a sodium leak occurs. In addition, liquid sodium can interact with structural materials, typically Fe-based austenitic and ferritic-martensitic (F/M) steels, leading to microstructural changes and property deteriorations.

Since the surface oxide layer can be readily reduced in liquid sodium, the primary corrosion concern for a liquid sodium environment is the dissolution of the alloy's metallic elements and an exchange of non-metallic elements between the alloy and the sodium [43]. Depending on the solubility of specific elements in sodium, the alloy's constituents can be dissolved uniformly or preferentially. The surface corrosion products can be eroded or spalled into flowing sodium, giving rise to various corrosion damage types such as mass loss, surface altered layers, intergranular attack, and carburization/decarburization. Figure 1 shows the solubilities of the constituent elements of typical stainless steels. At SFR operating temperatures, Ni is the most soluble in sodium, followed by Mn, Fe, Mo and Cr. With orders of magnitude higher solubility, Ni and Mn will preferentially leach out of SS, altering the surface composition. Since Ni and Mn are austenite stabilizers, their preferential leaching will also destabilize the surface microstructure. As a result, an altered surface layer featuring the ferrite phase can be observed on the areas wetted by sodium. While the effect of this selective leaching is relatively uniform near the surface, it is

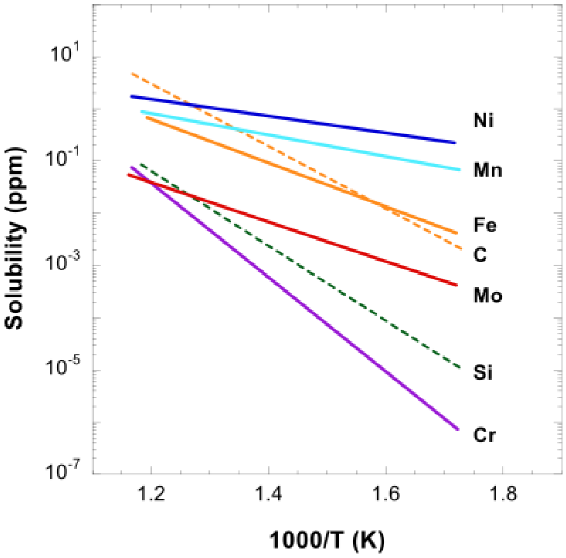

Figure 1. Solubility of alloy elements in liquid sodium, from Ref. [45].

more concentrated on grain boundaries deeper into the material. The depth of penetration of the surface alteration will depend on the activities of Ni or Mn in sodium.

The temperature gradient in a non-isothermal sodium system can create a condition of mass transfer through sodium flow. Alloying elements selectively leached from a hot section of the sodium system can subsequently be deposited to a cold section. Similarly, if different alloys are used to construct the sodium circulation system, the difference in chemical activity can also lead to mass transfers, altering the compositions and microstructures at both the hot and cold legs. For example, the surface of a ferritic (δ phase) oxide dispersion strengthened (ODS) steel was found to be changed with a Ni-rich γ phase in sodium [44]. In this case, the source of Ni was from the SS components of the same loop.

Non-metallic impurities such as oxygen in sodium can react with the material, affecting the dissolution of alloying elements. If liquid sodium contains sufficient oxygen, the dissolution rate of the alloy elements can become dependent on the formation energy of oxides in sodium. At temperatures relevant to SFRs, sodium chromate was observed to form with elevated oxygen content in sodium [46]. This reaction could increase the removal Cr from the alloy. Nonetheless, the effect of oxygen can be successfully managed with a cold trap method. The oxygen content can be lowered substantially in the system when the cold trap is operated < 150 °C, where oxygen can be precipitated out of liquid sodium [47].

The interactions between structural alloys and other non-metallic impurities in sodium are also of concern. Carbon is particularly important because of its critical role in SS and its relatively high solubility in liquid sodium. Depending on the activity, carbon can be transferred from one location to another in flowing sodium. In a single-material sodium system, carbon transfer manifests as a temperature-driven process, causing decarburization at the hot leg (the portion of the loop at high temperature) and carburization at the cold leg (the portion of the loop at a lower temperature). For an isothermal sodium system with different materials, carbon can be transferred from the high-activity material to the low-activity material. For example, in a system containing both ferritic and austenitic steels, the ferrite tends to be decarburized while the austenite tends to be carburized. The propensity of carburization or decarburization is sensitive to the carbide microstructure in the alloy. Ti- or Nb-stabilized SSs are more resistant to decarburization due to their low carbon activities, especially at high temperatures. The carburization/decarburization behavior is critical for the operation of SFRs because it can impact the microstructural stability and mechanical properties of the structural materials directly.

4.3.2 Lead-cooled fast reactors

A lead-cooled fast reactor (LFR)uses liquid lead (Pb) or lead-bismuth (Pb-Bi) eutectic as the coolant and operate around 480–650 °C. Compared with liquid sodium, liquid lead has a higher boiling point (1749 °C) and does not react aggressively with air or water. This could potentially simplify the cooling system design and permits a greater safety margin than that of SFRs. The structural materials of LFRs are also austenitic and ferritic-martensitic steels and nickel-based alloys.

Given the high solubilities of common steel alloying elements in Pb, mass transfers driven by activity differences will also occur in Pb or Pb-Bi systems. The difference between lead-based and sodium-based systems is that a stable oxide layer on the surface of structural materials does not exist in liquid sodium, but becomes possible in liquid lead. As a result, the dominant corrosion mechanism in Pb or Pb-Bi systems is oxidation [48]. To manage corrosion, an adequate level of oxygen needs to be controlled in liquid lead to form a passivation layer at the LFR operating temperature [49]. Too little oxygen is insufficient to form a protective layer, but too much oxygen will risk oxidizing liquid Pb. Thus, the corrosion issue concerning LFRs is a balance between oxidation and dissolution. The goal is to identify the conditions (temperature and oxygen activity) that enable a passivation layer. Since it is difficult to establish such a condition at high temperatures (above 550 °C), coatings have been proposed to modify the surface layer so that the temperature range of passivation may be expanded.

Another potential corrosion issue concerning Pb or Pb-Bi systems is liquid metal embrittlement (LME). For ferritic steels exposed to heavy liquid metals, embrittlement or significant loss of ductility is observed at temperatures up to approximately 400 °C [50]. The adsorption of heavy metals at crack tips or grain boundaries is hypothesized to be the mechanism weakening the bonding along the crack path. Since the interaction between stress and corrosion contributes to the adsorption of heavy metal atoms, LME is a form of environmentally assisted cracking (EAC) for LFRs.

4.4 High-Temperature Gas-Cooled Reactors

A high-temperature gas-cooled reactor (HTGR) uses helium gas as a coolant and a has very high outlet temperature exceeding 750 °C. HTGRs provide high efficiency in power generation and enable process heat applications such as hydrogen production [51]. With such high operating temperatures, typical structural steels do not have sufficient strength, and high-temperature nickel-based superalloys (e.g. Inconel 617), ceramics (e.g. graphite, SiC), or refractory metals must be used.

The corrosion issues concerning HTGRs arise from the impurities of helium gas. Small amounts of CO, CO_2, H_2, H_2O, CH_4 and N_2 are present in helium gas, leading to oxidation, carburization or decarburization of structural materials [48]. The oxidation of Ni-Cr alloys in helium containing impurities is controlled by Cr-H_2O and Cr-CO_2 reactions, all shown in Eqs. 1 and 2. The concentrations of H_2O and CO in helium are critical because they determine the oxygen partial pressure and carbon activity. It is important to maintain a slightly oxidizing condition so that a Cr_2O_3 film can be formed, although its integrity and protective nature might be challenged at very high temperatures [52].

$$2\mathrm{Cr} + 3\mathrm{H_2O} \longrightarrow 2\mathrm{Cr_2O_3} + +3\mathrm{H_2} \tag{1}$$

$$2\mathrm{Cr} + 3\mathrm{CO_2} \longrightarrow 2\mathrm{Cr_2O_3} + +3\mathrm{CO} \tag{2}$$

The presence of moisture and hydrogen in helium gas can also create conditions for decarbonization. As shown in Eqs. 3 and 4, the overall effect of the reactions between moisture and hydrogen with chromium oxide is to remove carbides while producing CO. The moisture and hydrogen involved are the media to facilitate these reactions.

$$2\mathrm{Cr_2O_3} + 6\mathrm{H_2} \longrightarrow 6\mathrm{H_20} + 4\mathrm{Cr} \tag{3}$$

$$2\mathrm{Cr_{23}C_6} + 6\mathrm{H_2O} \longrightarrow 23\mathrm{Cr} + 6\mathrm{CO} \tag{4}$$

Without the gas media of moisture and hydrogen, decarbonization could still occur in the solid state at the metal-oxide interface.

$$2\mathrm{Cr_2O_3} + 3\mathrm{C} \longrightarrow 2\mathrm{Cr} + 3\mathrm{CO} \tag{5}$$

Either through a gas medium or in the solid state, decarburization is a process that consumes the surface oxide layer and removes carbon from the alloy in the form of CO. As a result, decarburization could lead to a carbide-denuded zone near the surface underneath the oxide layer, reducing the strength of Ni-Cr alloys in the environment. On the other hand, if helium gas contains CH_4 or the partial pressure of CO is high, the alloy can undergo a carburization process, as shown in Eq. 6.

$$7\mathrm{Cr} + 3\mathrm{CH_4} \longrightarrow \mathrm{Cr_7C_3} + 6\mathrm{H_2} \tag{6}$$

Subsequent carbide-oxide reactions can follow, resulting in a porous surface scale. Carbides resulting from the carburization process can also become crack initiation sites, significantly reducing the tensile strength, cracking resistance, and creep performance of nickel alloys.

4.5 Small Modular Reactors

Unlike other types of reactors that can be characterized by their coolants and moderators, a small modular reactor (SMR) is a category of reactors with a variety of designs using different coolants and moderators [53]. The emphases of SMRs are on their small unit size and modularity. Depending on specific reactor designs, different materials will be selected to construct SMRs. As such, the corrosion systems (i.e., the material-environment combinations) concerning SMRs overlap with other reactor types. Some unique features of SMRs may influence specific corrosion issues to some extent. For example, the high grid compatibility of SMRs may impose a different requirement on their load-following capability, which may affect the EAC behavior of components in SMRs. However, since the reactor types utilized by SMRs are the same, no unique corrosion system specifically for SMRs is anticipated.

4.6 Corrosion Affected by Radiation

Corrosion behavior affected by irradiation is a concern across all reactor types. Since neutrons and other forms of radiation (e.g., gamma rays) are inevitable in the service environment near the reactor core, radiation-affected corrosion is an issue to be addressed when evaluating the corrosion behavior of reactor materials. Some topics, such as IASCC in LWRs, have been studied extensively [54], while other topics such as those concerning the concurrent irradiation and corrosion damage in MSRs have not been fully explored [55]. In general, radiation is considered a negative factor that reduces the corrosion resistance of structural materials due to the synergistic effects between radiation and corrosion systems [56]. However, in some special cases, radiation can also lead to less severe corrosion damage in structural materials [57].

The impact of radiation on corrosion arises from both its interactions with the material and the environment. By interacting with the material, radiation can change the material microstructure and microchemistry dramatically. Bombarded with energetic particles such as neutrons, protons, and alpha particles, lattice atoms in a metal can be displaced from their regular sites, leaving behind a large number of interstitials, vacancies, and defect clusters. The subsequent evolution of these defects give rise to irradiation effects such as dislocation microstructure, radiation-enhanced diffusion, and radiation-induced segregation (RIS). The resulting microstructural and microchemical changes in irradiated materials can certainly contribute to their corrosion responses. A well-known example of a radiation-affected corrosion phenomenon is the Cr depletion at grain boundaries in Fe-Cr-Ni alloys [58]. RIS induces an inverse Kirkendall effect that reduces the Cr concentration while increasing the Ni concentration at grain boundary. The decline in Cr concentration affects the passivation of grain boundaries, elevating the vulnerability of intergranular corrosion attack. Similar effects can also be observed on material surfaces, where Ni and Si enrichment and Cr depletion are often detected [59]. This influence of radiation on corrosion can affect all reactor types as long as irradiation-induced microstructure and microchemistry persist in reactor materials.

In addition to microstructural changes, radiation can also cause changes in corrosive environments. While atomic displacements may not be a concern for reactor coolants, which are either a liquid or gas, radiation can still interact with electrons in the corrosive medium, making radical species that can be more corrosive to alloys [56]. An example of such an effect is the radiolysis of water, in which water molecules are transformed into H_2, O_2, and H_2O_2 under ionizing radiation, significantly elevating the electrochemical potential of SS in water [60]. The effect of radiolysis may not be important for molten salts since they consist of dissociated anions and cations. However, acceleration or deceleration of corrosion can occur under proton irradiation in molten salts [57, 61], suggesting a dynamic interaction between RIS and the corrosive environment. Regardless the true mechanism(s) of altered corrosion rates, the impact of radiation on corrosive environments is transient and will not exist without radiation during the corrosion process.

4.7 Summary and Conclusions

The scope of corrosion is wide for the entire field of advanced reactors; each reactor type has its own reactor-specific corrosion concern. The Advanced Materials Manufacturing Technologies (AMMT) program must prioritize the material-environment systems to test to make the most impact with its available funding. As discussed in Chapter 1, the AMMT program will focus first on additively manufactured (AM) 316H material. Given the intended service application of 316H, corrosive environments at high temperatures are prioritized, as are advanced reactor types with the least information available. As a result, the priority list for environment testing is

- Molten chloride environments
- Liquid sodium environments
- Molten fluoride environments
- High-temperature helium environments
- Liquid lead environments
- Other advanced reactor environments (supercritical water, carbon dioxide)
- Light water reactor environments.

It is important to note that light water reactor environments are generally considered other under Department of Energy, Office of Nuclear Energy (DOE-NE) programs, and therefore will not be studied unless a specific need or directive arises. In addition, corrosion testing should occur in a staged fashion: first, on unirradiated material in laboratory (radiation-free) environments; then, testing of irradiated material in radiation-free environments; and finally, *in situ* or in-reactor irradiation testing to provide prototypical results and to probe synergistic effects between the radiation environment and the material. Testing of ion-irradiated material should be considered as a potential means of investigating the impact of radiation-induced microstructure evolution on corrosion behavior; however, the results will necessarily be focused on understanding corrosion mechanisms due to the small sample volumes achievable.

5. KEY FACTORS LIKELY TO INFLUENCE CORROSION PROPERTIES OF ADDITIVELY MANUFACTURED MATERIALS

Due to the very different fabrication methods, as-fabricated additively manufactured (AM) components are different from conventionally manufactured components both in terms of microstructure and as-fabricated surface finish. The corrosion behavior of AM components can vary significantly from that of conventionally formed components as a result of these differences. Characteristics of AM materials such as surface roughness, porosity, inhomogeneous microstructure, and residual stress may have profound impact on their service performance, and therefore AM-specific corrosion issues need to be identified in the effort of advancing corrosion research on AM materials.

5.1 Bulk Phenomena

Laser-based AM techniques, such as laser powder-bed fusion, produce heterogeneous and anisotropic microstructures due to the layer-by-layer nature of the manufacturing process coupled with rapid solidification and large spatial thermal gradients. In laser powder bed fusion (LPBF) 316L, the intrinsic, multiscale chemical heterogeneities (such as solute segregation, chromium depletion, and precipitate formation) inevitably alter the corrosion performance.

5.1.1 Residual stress

Residual stresses from the build process can be significant enough to cause visible warping of as-built components upon release from a build plate. Laser-based AM processes can result in very high thermal gradients locally; combined with rapid cooling and repeated heating from layer-by-layer building, residual stresses can be significant in as-built AM components. These stresses tend to be compressive inside AM components and tensile on the component surface [62]. Residual stresses are often highest along the build direction. In addition to causing geometrical problems such as distortion or delamination, residual stresses are known to impact passivity [25] and environmentally assisted cracking (EAC) susceptibility [63], especially when the stresses are in tension and above the yield stress. Due to the critical role of residual stress in AM material performance, process strategies such as scanning pattern and temperature control can help manage residual stresses. More importantly, post-build heat treatment is frequently necessary to relieve residual stresses, which should mitigate the impact on the corrosion performance. While residual stress may not be a unique problem for AM materials, it can cause a significant impact on the corrosion performance. As a result, particular attention needs to be paid to managing residual stresses and minimizing their impact on the corrosion resistance of AM materials.

5.1.2 Porosity

Build porosity is also a concern, with pore volume fractions of 5% or more possible depending on processing parameters [64], although full density is typically targeted. As a matter of course, AM materials contain defects such as microscale pores or larger lack-of-fusion cavities. While both types of defects are empty voids within an otherwise sound solid, they show distinct morphologies (e.g., irregular, ellipsoidal, or spherical) and have different origins (e.g., from trapped gas or partially melted powder). The overall quantity of these defects can be measured by the porosity level. AM processing parameters such as the energy density of the laser beam and the feedstock properties can influence the porosity level considerably. Mechanically, pores or cavities are stress risers, which can facilitate crack initiation. Chemically, they are vulnerable sites for pitting or other forms of localized corrosion if a corrosive medium is present. Lack-of-fusion cavities can provide crevice-like occluded areas that promote the development of aggressive corrosion chemistry [65]. The effect of porosity on SCC susceptibility is not clear at present. While a study on cold-worked AM materials seems to show a positive correlation between porosity and stress corrosion cracking (SCC) susceptibility [10], another study with as-printed materials containing low porosity did not show any effect of porosity on SCC [11]. Regardless, porosity is a characteristic of AM materials, and the influence of porosity on corrosion should be treated as an AM-specific corrosion issue.

The metastable pitting characteristics of AM selective laser melting (SLM) 316L stainless steel (SS) of different porosities were compared with wrought 316L SS using potentiostatic testing [66]. The number of metastable pitting events were normalized to surface area and exposure time to obtain a pit formation frequency. In addition, the pitting potential and corrosion potential were measured. A pitting potential is defined as the potential at which the protective passive coating breaks down and the characteristic of the electrochemical system becomes transpassive. The test results showed that the porosity of AM SLM 316L does affect the metastable pit formation frequency, although the measurement of pitting potentials of SLM 316L shows large standard deviations. However, as an overall trend, the pitting potential of SLM 316L is improved over wrought 316L even at the highest pit formation rate. Conversely, the corrosion potentials do not show noticeable differences. SLM 316L shows significantly higher pitting potential than the wrought SS316L but very similar corrosion potentials. The corrosion potential did not show a clear trend with porosity and the corrosion current densities of the SLM samples were somewhat higher than those of the wrought counterparts.

5.1.3 Heterogeneous and anisotropic microstructures

The microstructure of AM materials is generally complex. Unlike traditionally manufactured materials, AM materials have a complex solidification microstructure. The details depend on the material and process, but melt pool boundaries are generally visible at the macroscale in fusion-based methods and individual grains (defined by high-angle grain boundaries) are generally elongated along the thermal gradient present during the build process. Within each grain, a cellular dislocation structure generally occurs during AM builds of stainless steels and other metals [12], similar to the dislocation cell structure that occurs during plastic deformation and may also have solute segregation to the cell walls. Additionally, other phases may be present in AM material that are not present in conventional material of the same composition. Oxide phases or atypical inclusions may be present in AM material due to feedstock oxidation or other contamination, while previously unreported phases may occur as a result of the rapid cooling and repeated thermal cycling in AM build processes.

Related to the solidification process, AM materials often exhibit columnar or irregular grain structures or textures [65]. Grain growth following the solidification of the melt pool tends to be along a certain crystallographic orientation. The resulting texture depends on the thermal gradient and the solidification rate, and therefore can be controlled by process parameters. Scan strategies giving rise to more homogeneous melting and solidification reduce the extent of printing texture [65]. The presence of an anisotropic grain structure can influence corrosion properties such as pitting, localized corrosion [62], and SCC susceptibility [10]. While anisotropic grains are certainly not a unique issue for AM materials, it is a specific issue to be addressed when corrosion performance is of concern. Several studies have demonstrated that process controls can minimize the detrimental effects of anisotropic grain structure on the corrosion performance of AM materials.

The microstructure and corrosion resistance of 316L samples prepared using SLM and laser metal deposition (LMD) were compared with those of wrought material [24]. During fabrication, SLM created smaller melt pools and produced much finer cellular microstructures than LMD, which was found to affect the corrosion properties of AM 316L. The mean grain size of wrought 316L is about 20–30 μm coarser than the cell sizes in the microstructures of LMD 316L and SLM 316L (about 4 μm and 0.7 μm, respectively). Different manufacturing conditions produced materials of different microstructures but fairly similar corrosion potential and passive current density values, though the passivation potential was strongly impacted. The passivation potentials of the materials, however, show variations in the order SLM material $>$ LMD material $>$ wrought material. The results imply that with finer microstructures, the passivation surface layer of stainless steel is maintained at far higher potentials until the passivation layer breaks down and the system becomes transpassive. Therefore, AM SLM 316L showed the highest (most noble) passivation potential associated with its finer microstructure, thought to lead to a more stable protective oxide [24].

Intergranular and intragranular Si- and Mn-rich oxide inclusions are present in laser AM austenitic stainless steel. Alloying elements such as manganese, molybdenum, and silicon have a strong affinity to oxygen and will form oxide particles. Silicon-rich oxide inclusions in AM 316L SS will reduce impact toughness and SCC properties. The intragranular oxide inclusions promote early microvoid formation to reduce the impact toughness relative to materials fabricated by powder metallurgy-hot isostatic pressing (PM-HIP) and wrought materials, of comparable grain sizes [67]. A higher volume fraction of oxide inclusions is expected to reduce the impact toughness and increase the SCC susceptibility of AM materials in high-temperature water [67].

The higher oxygen concentrations of AM materials, relative to wrought alloys, are a result of adsorbed oxygen in the alloy feedstock powder. During manufacturing, micrometer-size oxides with Mn, Mo, or Si form. The uniform oxide dispersions in AM materials may disrupt the continuity of the passivating film, impacting its corrosion behavior. The control of oxygen and high oxygen-affinity elements like Si during advanced manufacturing may help to reduce oxide formation. Further studies are needed to enhance the understanding of process-related oxide formation. AM powder feedstock should undergo rigorous quality control to ensure as low as possible oxygen surface concentration, and suitable protocols must therefore be established.

5.1.4 Cellular substructure and segregation

For the composition of 316 SS, dendritic growth prevails during solidification, giving rise to solute segregation (e.g., Ni, Cr) and a dislocation cell structure. This cellular substructure is on the order of 1 μm in size, although it varies depending on the build parameters. The dislocation cell structure consists of cell walls on the order of tens of nanometers thick, composed of tangled dislocations and relatively dislocation-free cell interiors. The dislocation cells are generally columnar in nature with the small dimensions approximately equal, rather than equiaxed in all three dimensions. The cellular microstructure of AM 316L has a non-equilibrium nature and shows enrichments of mostly all alloying constituents–Cr, Ni, Mo, Mn, and Si–at the microstructure cell wall, while the cell center, as a result is incomplete solutionizing, is enriched with iron.

This unique heterogeneous microstructure can have important implications on the corrosion behavior. In a biological environment, a dislocation cell structure was found to improve the passivating behavior by providing a high density of oxide nucleation sites [68]. However, results are mixed and defects can become a dominant factor for the corrosion response [69]. We can assume galvanic coupling occurs between the iron-rich cell center and the more noble cell wall. Solute-depleted cell interiors could undergo preferential attack in oxidizing environments with the iron acting as sacrificial anode, electrochemically protecting the more noble cell wall with relative higher concentrations of Cr, Ni, Mo, Mn, and Si. Without solution annealing, the corrosion of iron in AM 316L would therefore be enhanced. Since the heterogeneous microstructure originates from solidification, AM process parameters influencing the heating and cooling of the melt pool and overall build are important. For example, the extent of solute segregation can be controlled by altering the scan speed [70]. Furthermore, if the solidification microstructure contains δ-ferrite, this microstructural inhomogeneity could also alter the corrosion response [71]. As shown in numerous studies, the inhomogeneous microstructure resulting from solidification process can impact the corrosion behavior of AM materials. As a result, this AM-specific corrosion issue must be characterized and understood.

Additive manufacturing process parameters are important for the corrosion performance of AM materials. Specimens of AM LPBF 316L were produced at print speeds of 550-, 650-, and 700-mm s^{-1} and their corrosion potentials and corrosion current densities were measured [72]. With increasing print speed, dislocation structures become more pronounced. An increase in printing speed from 550 to 700 mm s^{-1} promotes finer microstructures, decreases the average lattice parameter, and increases dislocation densities. Higher printing speeds promote enhanced solidification rates within a single print track, affecting the solidification microstructure. Consistently, the largest lattice contraction and dislocation density was reported for the specimens printed at 700 mm s^{-1} [72]. The reduction in lattice parameter is driven by dealloying and chromium depletion from the austenite matrix phase, resulting in chromium segregation to the boundaries of the cellular microstructures. The increased dislocation density induces some changes in corrosion potentials measured by cyclic voltammetry. Samples printed at higher speed show larger hysteresis eventually derived from disruption of the passive oxide film layer with subsequent stable pit growth, and hence an elevated anodic current until repassivation conditions are reached [72]. Corrosion and pitting potentials move slightly to the more noble region, but data scattering is too large to formulate a solid quantitative statement about how the dislocation structure impacts electrochemical potentials.

Faster scan speeds and a more pronounced dislocation structure can lower pitting potential and increase the susceptibility for pitting corrosion compared with wrought counterparts, but reverse effects are also possible [72]. Overall, data scattering is large. The repassivation potentials of LPBF 316L produced at low printing speed are lower than those of wrought 316L, while at high printing speed and high-defect densities the data scattering is too high for quantitative statements. It seems obvious that the reproducibility of dislocation structure at high scan speeds is low and data scattering is therefore high, diminishing the quality of any trend quantifications.

For now, it is fair to state that increasing the dislocation densities produces lower (less noble) corrosion potentials of LPBF 316L and lower passivation current densities. Wrought SS316L shows corrosion potentials similar to the specimens produced at 650 mm s^{-1} combined with low passivation current densities like the 700-mm s^{-1} specimens. In the AM fabrication process, low print speed enables more noble corrosion potentials but far larger passivation current densities.

5.2 Surface Phenomena

The corrosion behavior of AM components is subject to its surface finish. While traditionally fabricated components generally have a machined surface, one benefit of AM processing is building net or near-net shape components; without post-build surface machining, surface roughness created by the AM process is a macroscopic concern. AM surfaces typically have roughness on the order of the feed powder or metal wire used during the build. For example, the surface roughness for components produced via SLM are in the range of 10 μm to 30 μm [21], and are about 1 order in magnitude larger than the surface roughness of parts produced by conventional manufacturing, for example, by milling (0.8 μm), honing (0.1 μm), or lapping (0.05 μm). This roughness may be sufficient to promote localized crevice corrosion. Another concern is porosity intersecting the surface (or just under the surface, to be revealed after some amount of uniform corrosion) and is another source of possible crevice corrosion initiation. In addition, AM surface features such as balling (droplets), staircasing (surface curvature), and partially fused powder particles can result crevice-like defects. The formation of surface defects depends on the angle and orientation of the printed piece during printing, and some surfaces are rougher than others. It is also affected by printing parameters such as the energy density of the energy source and the hatch distance. Surface remelting can reduce roughness on the top surfaces but may not help the inclined surfaces.

The effect of surface roughness on the corrosion behavior of 316L SS manufactured by LPBF was studied by surface grinding samples to reduce the surface roughness from 2.8 ± 0.6 μm to 0.07 ± 0.04 μm. Three different corrosion environments were used: 3.5 wt% NaCl water solution, 3 wt% H_2SO_4 solution, and high-temperature oxidation at 800 °C. Decreasing the surface roughness of AM LPBF 316L has a significant impact on the electrochemical behavior and therefore on the material's corrosion properties. Reducing the surface roughness reduced the corrosion current densities and shifted the corrosion potential in the positive (more noble) direction. The surface-treated specimens, because of improved passivation layers, showed higher corrosion resistance, while in electrochemical tests the as-built LPBF 316L showed less corrosion resistance. In high-temperature oxidation experiments, the lowest mass gain was found in the surface-treated specimens [73]. Overall, surface finish is a key factor contributing to the corrosion performance of AM materials, and should be carefully characterized and managed to assure adequate corrosion resistance in service environment.

5.3 Post-Build Treatments and Process Variability

Given the features of AM materials (surface roughness, solute segregation, complex microstructure, and residual stresses), some amount of post-build processing generally occurs. The surface may be machined, as previously discussed. Post-build annealing is also common for stress relief, solution annealing, or microstructure homogenization [4]. However, post-build processing incurs additional time and cost, and it generally will not resolve the presence of additional oxide phases, atypical inclusions, and build porosity, and may or may not remove the original build microstructure.

The impact of the unique microstructural features of AM 316L SS on corrosion fatigue behavior was studied for high-temperature water under boiling water reactor/pressurized water reactor (BWR/PWR)-type oxidizing conditions [10]. AM LPBF 316L SS was heat treated to produce variations in microstructure and residual plastic strain. Three different heat treatment conditions were used to assess the effects of microstructure variations on the corrosion fatigue crack growth behavior: (1) stress relief at 650 °C for 2 hours in argon, (2) HIP for 4 hours at 1150 °C and 100 MPa in argon, and (3) heat treatment at 955 °C for 4 hours in argon. After appropriate heat treatment, LPBF 316L can exhibit a corrosion fatigue crack growth response in high-temperature water similar to that of its wrought counterpart [10]. However, hot isostatic pressing (HIP) treatment did not make a significant improvement over the stress-relieved condition regarding porosity. Solution annealing (955 °C for 4 hours) was selected to produce a bimodal microstructure involving both recrystallized equiaxed grain and as-built characteristics. Full recrystallization, however, was not always achieved due to the strain variations at different locations of the as-built part and some un-recrystallized grains remained [10].

Cold-worked stainless steels are known to be susceptible to corrosion fatigue and SCC in high-temperature water typically for BWR or PWR nuclear reactor conditions. The as-built material cold-worked in different directions resulted in different crack growth rates. Stress-relieved AM 316L SS exhibited a far higher crack propagation rate along the build direction than normal to the build direction. Stress-relieved AM 316L SS cold-worked along the build direction resulted in similar crack propagation rates to cold-worked AM 316L SS that had undergone HIP and solution annealing. This orientation dependency in stress-relieved material is explained by its anisotropic microstructure [10]. As the load frequency decreased in the corrosion fatigue tests, the impact of environment became more dominant in the corrosion process and corrosion fatigue increased significantly. Wrought 316L stainless steel showed lower corrosion fatigue rates than AM LPBF after being stress relieved and after HIP and solution annealing. Especially at low-load frequencies, crack growth rates of stress-relieved AM LPBF 316L are more than twice the crack growth rates measured in wrought 316L SS.

Process variability impact on AM material properties is a significant concern and extends to their corrosion behavior. In this context, process variability refers to variations in the as-built microstructure from a single, specific machine. Even with the same build parameters in the same AM machine (e.g., laser power, scan pattern, and speed for laser powder bed fusion), sources of process variability include, but are not limited to, the laser power and scan speed; feedstock lots; atmospheric storage condition of the feedstock, especially powder feedstock; atmospheric composition during the build, including humidity levels [74]; and heat dissipation during the build as a result of build plate heating, surrounding atmosphere, and build geometry. The geometry of the as-built specimen from which corrosion samples are removed should be considered part of process variability. It is conceivable to take corrosion specimens from short specimens with limited build volume, while the actual component will be larger. Given the impact of build volume on thermal history and resulting microstructure, corrosion specimens sectioned from specimens of representative geometries and volumes of the actual component may also need to be assessed.

5.4 Additively Manufactured Material Characteristics to Measure and Quantify

Within AMMT, corrosion research on AM materials will be focusing on AM 316 due to its potential applications in a wide range of reactor concepts. Since the composition of AM 316 is similar to that of traditionally manufactured 316 SS, no fundamentally different corrosion mechanism is anticipated. Corrosion issues affecting traditionally produced 316 SS in different reactor environments should occur as well in AM 316 SS. Thus, it is anticipated that corrosion tests performed with AM 316 SS should be no different from those performed with traditional materials. The basic corrosion behavior of AM materials can be characterized with immersion or electrochemical tests, and the service performance can be evaluated with mechanically assisted corrosion tests. Despite similarities between AM and traditional materials, AM materials do have specific issues concerning their corrosion performance. Precautions are needed to characterize AM materials and evaluate their corrosion degradation properly.

First, AM materials have unique surface finishes resulting from the printing process, which may strongly influence the corrosion behavior. Depending on the objective of a corrosion test, the surface effect needs either to be analyzed quantitively or eliminated. If the goal is to understand the bulk response of AM samples to corrosive environment, for example the SCC performance of an AM material, the effect of the surface should be eliminated. The as-printed surface layer should be removed and polished to a specified finish to ensure consistency in testing. If the goal is to investigate the impact of different as-printed surface finishes on corrosion behavior, the sample's surface condition should be characterized quantitatively before and after the corrosion tests, so that a correlation can be established between surface finishing and corrosion response. Standard microscopy or a roughness measurement can be performed to characterize the AM sample surface.

AM materials also contain microscale pores that can impact their corrosion behavior. Since porosity is a common AM feature affecting almost all properties of AM materials, it is often characterized thoroughly with various techniques. Metallurgical methods such as optical and electron microscopy, density measurement, or X-ray tomography have been used to characterize porosity in AM materials [68]. The porosity information can be utilized to understand the corrosion behavior of AM material and assess their performance in reactor service environment. Furthermore, AM processes may result in anisotropic grains and large residual stresses in specimens. These characteristics of AM materials will have a strong influence on their service performance since anisotropic corrosion behavior may arise or stress-enhanced corrosion attack may occur without warning. Corrosion research on the performance of AM material should focus on these effects and quantify their impact if possible. Again, basic metallographic techniques can be used to characterize AM material's anisotropic grain structure, and post-built heat treatments may be applied to minimize the impact of residual stress.

For the corrosion properties of AM materials, the most important effect arises from the microstructural and compositional inhomogeneities. As discussed previously, AM microstructures are significantly different from those of traditionally made materials. Repeated heating and rapid cooling during the AM process creates inhomogeneous microstructures featuring dislocation cells and solute segregation. This microscale inhomogeneity can lead to a local corrosion attack such as pitting. As such, a good understanding on the inhomogeneity of the AM materials is critical to understand and predict the corrosion behavior of AM materials. Microstructure characterizations such as transmission electron microscopy and energy dispersive spectroscopy are necessary to acquire detailed information about the inhomogeneous microstructure to analyze its influence on corrosion properties. Cellular structure including dislocation density, cell size, and microsegregation should be measured. Finally, all those AM-specific corrosion issues could increase the uncertainties of the corrosion responses. As a result, multiple samples and repeated measurements under the same conditions may be needed to achieve the same level of statistical significance of experimental results.

5.5 Summary and Conclusions

Both bulk properties and surface properties of an AM material can impact its corrosion performance. Thus, several features of AM material can impact corrosion behavior: for example, the surface roughness and porosity may contribute to crevice corrosion; dislocation cell structure, chemical segregation, and atypical phases and inclusions could promote galvanic corrosion (including pitting) or leaching; lamellar or columnar grain structures and melt pool boundaries could lead to exfoliation; and residual stresses could change the pitting potential. The orientation of a corrosion coupon (e.g., along the build direction) will thus be important to assess. Surface roughness and post-build surface re-finishing can impact component corrosion, especially crevice corrosion, as can the intersection of build porosity with the surface. Process variability and variation in corrosion coupon microstructure due to sampling location from the build geometry should also be assessed.

6. EXPERIMENTAL CAPABILITIES REQUIRED FOR CORROSION RESEARCH OF ADDITIVELY MANUFACTURED ALLOYS

To characterize the corrosion behavior of materials, various test methods may be used to evaluate the extent of a corrosive attack. These tests can be as simple as measuring the sample's weight and thickness changes after exposure to a corrosive environment, or as complex as *in situ* monitoring of crack development under simultaneous corrosion attack and thermomechanical degradation. Regardless of the complexity of the experimental methods, the purpose of corrosion testing is to reveal the nature of the corrosive attack and to quantify the extent of material deterioration in a specific corrosive environment.

6.1 Types of Corrosion Tests

Corrosion test methods can be broadly categorized into three types: immersion (including static and flowing fluid), electrochemical, and mechanically assisted or irradiation-assisted tests. For laboratory corrosion tests, the samples are usually small and their surface conditions can be effectively controlled. The corrosive environments relevant to nuclear applications include water, liquid metals, molten salts, and helium with impurities. Since elevated temperatures and pressures are present in reactors, autoclaves are often needed to simulate reactor service environments.

6.1.1 Immersion tests

Static immersion (capsule) tests provide a measure of the general corrosion behavior and are a good screening method to eliminate materials that are incompatible with the test environment. Small coupon specimens prepared from the materials of interest are exposed to the test environment, and the weight and thickness changes of the specimens are measured as a function of exposure time. Weight measurements are used to determine weight loss or weight gain of the sample, indicating removal of material or addition of material (often oxide formation). Thickness measurements provide similar information about material loss or gain. In addition to weight and thickness measurements, other characterization techniques can be used for post-exposure examination of immersed samples. Optical and electron microscopy can provide information on the surface morphology and the nature of the surface layer, which is valuable to understand the underlying mechanisms. In addition, immersion tests can also be performed with stressed samples. Static loading can be readily implemented in immersion tests with U-bent or C-ring specimens [23], simulating the corrosion conditions favorable for stress corrosion cracking (SCC) initiation.

Flowing immersion tests are typically executed as loops. These tests simulate real-world scenarios where materials are exposed to corrosive environments while the fluid is flowing (e.g., coolant flowing through pipes or heat exchangers). The fluid flow rate can be adjusted to simulate specific operating conditions. One major difference between static tests and flowing tests is that the corrosion rate in static tests will decrease as corrosion progresses due to saturation of species in the fluid. However, loop tests with a hot leg (the portion of the loop with the sample) and a cold leg (the portion of the loop without the sample and at a lower temperature) will typically result in deposition of the material in solution at the cold leg due to increased solubility, ensuring the corrosion process continues at a high rate.

Both static and flowing tests are sensitive to the choice of capsule or loop material. The capsule or loop material should be inert with respect to the corrosive environment and should also be compatible with the sample material. For example, the capsule material should have negligible solubility for elements within the sample material; otherwise an inadvertent corrosion cell could be created.

6.1.2 Electrochemical tests

Electrochemical tests are focused on the control and measurement of the fundamentals of electrochemical reactions and are used to assess a material's corrosion resistance and passivation properties. Using the electrical current, potential, and resistance properties of the electrochemical cell, these tests can provide insights into how materials respond to oxidation and reduction processes. The electrochemical potential is a good measure of the driving force of the reactions that occur at the anode and the cathode, and the current density is an excellent representation of the rate of the reaction. Based on the principle of the electrochemical cell, several types of electrochemical tests can be developed, including potential, resistance, current, and polarization measurements [23]. These tests can be used to determine the galvanic series, the level of cathodic protection, the corrosion rate, the susceptibility to pitting, etc. These fundamental corrosion properties can help develop corrosion-control strategies and implementations.

6.1.3 Assisted corrosion tests

Mechanically assisted corrosion tests are particularly important for approximating the conditions encountered in service since they emulate the simultaneous presence of mechanical loading and a corrosive medium. While immersion and electrochemical tests can emulate a well-defined material-environment system adequately, mechanical damage that may influence the corrosion deterioration is not evaluated. Except for some limited cases, the effects of mechanical loading on the development of corrosion degradation is not considered in immersion or electrochemical tests. In real-world applications however, the synergistic effects arising from the interaction of corrosion and mechanical degradation are often the controlling factors for the most dangerous form of corrosion attack, such as SCC or corrosion fatigue. Mechanically assisted corrosion tests are designed to represent these types of service conditions closely and to measure the material properties directly related to the failure mode. For example, if cracking is the expected failure mode, fracture mechanics properties such as crack growth rate or fracture toughness are measured. Although these tests are more complex experimentally, the information they can provide is highly relevant to the service performance.

Irradiation-assisted corrosion tests aim to explore the synergy between two damage mechanisms—radiation and corrosion. As shown in Chapter 4.6, radiation exerts its influence on corrosion both by modifying the material microstructure and changing the chemistry of the environment. When the effects of radiation-induced microstructure evolution is of interest, the material irradiation and corrosion testing can be performed sequentially because the irradiated microstructure persists beyond the end of the irradiation. From a technical standpoint, the corrosion tests performed with irradiated materials and unirradiated materials are the same, except for additional challenges posed by radiological specimens. However, when the effect of radiation on the corrosive environment (e.g. radiolysis) is the focus, the corrosion test must be performed with simultaneous irradiation because of the need to capture the dynamic interaction between the ionizing radiation and the corrosive medium. Although radiation-assisted corrosion tests are difficult to perform, they can provide important insights into the unique degradation mechanisms that materials may experience in reactor service environments.

6.2 Available Facilities Accessible to Advanced Materials Manufacturing Technologies

Various test facilities are available across Department of Energy (DOE) laboratories to evaluate the impact of corrosion on additively manufactured (AM) materials. As part of the current effort, a survey was conducted at Argonne National Laboratory (ANL), Idaho National Laboratory (INL), Oak Ridge National Laboratory (ORNL), and Pacific Northwest National Laboratory (PNNL) to understand the available experimental capabilities that can be utilized to meet Advanced Materials Manufacturing Technologies (AMMT) testing needs. Since corrosion research encompasses a vast and diverse range of topics, a comprehensive summary on all experimental capabilities relevant to corrosion research are not possible. The survey was limited to the research groups currently working on nuclear structural materials and emphasized reactor-specific testing capabilities. While general corrosion testing capabilities are widely available in chemical and metallurgical laboratories, reactor-specific testing facilities are scarce and more difficult to access because of the reactor service conditions they intend to emulate. Compared with the general evaluation of corrosion properties, reactor-specific testing is more likely to provide information directly useful for the adoption of AM technologies by the nuclear industry.

The survey results of the four laboratories are compiled in Tables 3 - 6. The types of experimental work that can be performed and the relevant reactor types are specified. The lists of materials that have been evaluated in these laboratories are not exhaustive; the intention is to show the relevance to the corrosion systems to be addressed. The ability to handle radioactive materials varies among these facilities, and most of them do not evaluate neutron-irradiated specimens that contain irradiated microstructures. However, INL has extensive facilities such as the Irradiated Materials Characterization Laboratory to handle highly radioactive specimens with state-of-the-art materials science techniques. For those facilities that can test radioactive materials, the acceptable radiation and contamination levels have not been assessed, and they can

Table 3. Experimental facilities at ANL used for corrosion research on reactor materials.

Facility	Type of experiments	Applicable reactor types	Materials
Irradiated materials laboratory	IASCC, corrosion fatigue crack growth, hydrogen embrittlement	LWR	SS, F/M steels, Ni alloys, Zr alloys
Stress corrosion cracking	SCC, corrosion fatigue crack growth, hydrogen embrittlement	LWR	SS, Ni alloys
Environmentally assisted fatigue, creep fatigue	Environmental fatigue, creep fatigue	LWR, SFR, HTGR	SS, Ni alloys, F/M steels
Environmental creep	Creep test in controlled gas environment	HTGR	SS, Ni alloys, F/M steels
High Pressure Testing Facility	Component testing	LWR	SS, Ni alloys
Sodium materials test loops	Mass transfer in sodium, carbonization and decarbonization evaluation	SFR	SS, F/M steels

also vary over time based on local policies and radiological controls. Because of the ambiguity of the information, specific radiological facilities (or “hot” laboratories) are not identified.

Basic characterization capabilities for studying the fundamentals of corrosion behavior exist across all laboratories. Standard immersion and electrochemical tests are routinely performed in regular laboratories. Testing in highly hazardous corrosive environments such as liquid metals and molten salts are more difficult and therefore the availability of testing facilities decreases. Thanks to previous investments by various DOE programs, the testing facilities available to AMMT cover all reactor environments. As shown in Fig. 2, the light water environment has the best availability in terms of reactor-specific testing capabilities. About 40% of these test facilities can perform corrosion tests in light water reactor (LWR) environments. The second most supported environment is liquid sodium, where roughly one quarter of the test facilities can conduct corrosion tests related to liquid sodium. Molten salts test facilities are also available with somewhat limited accessibility. Overall, there is a good availability for reactor-specific corrosion testing capabilities among the national laboratories. Almost all corrosion systems defined by the material and environment of interest are covered among the testing facilities in this survey.

Table 4. Experimental facilities at INL used for corrosion research on reactor materials.

Facility	**Type of experiments**	**Applicable reactor types**	**Materials**
Aqueous Static Corrosion Testing Facility	Static corrosion testing facility in water	Water-cooled reactor, LWR	Stainless steel, Ni-based alloy, alloy 709, high-entropy alloy, etc.
Molten Salt Static Corrosion Testing Facility	High temperature static corrosion tests under inert environment	Chloride and fluoride-salts based MSRs	Stainless steel, Ni-based alloy, alloy 709, high-entropy alloy, etc.
Molten Salt Galvanic Corrosion Testing Facility	High temperature galvanic corrosion tests between different materials under inert environment	Chloride and fluoride-salts based MSRs	Graphite/structural material alloy coupling, different structural material alloy coupling, i.e., stainless steel, Ni-based, alloy 709, high-entropy alloy, etc.
in situ High Temperature Testing under stress	High temperature static corrosion tests under inert environment, using three- or four-point stress benders	Chloride and fluoride-salts based MSRs	Structural material alloys, i.e., Stainless steel, Ni-based alloy, alloy 709, high-entropy alloy, etc.
Molten Sodium Static Corrosion Testing Facility	High temperature static corrosion tests under inert environment	SFR	Structural material alloys, i.e., Stainless steel, Ni-based alloy, alloy 709, high-entropy alloy, etc.

Table 5. Experimental facilities at ORNL used for corrosion research on reactor materials.

Facility	**Type of experiments**	**Applicable reactor types**	**Materials**
Water Loop	High pressure water loop up to 330 °C, 2200 psi, <50ppb dissolved oxygen	LWRs	SS, FeCrAl, SiC
Liquid Metals (LM) Compatibility	Capsule test and thermal convection loop in Na, Pb, etc. (corrosion rate, mass transfer)	SFR, LFR	Ferritic/martensitic, SS, Ni-based alloys
Molten Salt Compatibility	Capsule test and/or thermal convection loop in $KCl-MgCl_2$, FLiNaK, FLiBe, etc. + Salt purification system	MSR	SS, Ni-based alloys
High Temperature Cyclic Oxidation	TGA and cyclic oxidation testing in controlled environments up to 1500°C	HTGR	F/M, SS and Ni-based alloys
Environmental tensile, creep, fatigue & creep fatigue	Creep, fatigue and creep-fatigue testing in controlled environments (H_2, He, Steam, CO_2, etc.)	LWR, HTGR	F/M, SS, Ni-based alloys
Tensile, creep, fatigue & creep fatigue in LM and MS	Creep, fatigue and creep-fatigue testing with cylindrical specimens filled with LM or MS	SFR, LFR, MSR	SS and Ni-based alloys
Severe Accident Test Station	Cladding burst testing in controlled atmosphere at high temperature	LWR	Zr alloy, FeCrAl
Supercritical CO_2	Autoclaves up to 800°C, 300 bar	CO_2	F/M, SS, Ni-based alloys

Table 6. Experimental facilities at PNNL used for corrosion research on reactor materials.

Facility	Type of experiments	Applicable reactor types	Materials
Corrosion Lab	Multimodal corrosion setup, Stress induced corrosion tests	LWR, SFR	SS, Al, Steel (Automotive, Naval Steels), joints and interfaces, Boehmited & coated surfaces
Mechanical Test Lab	Thermal and fatigue stress corrosion	LWR, SFR	Coatings and joint interfaces.
Rad-Test Lab	High temperature aqueous corrosion testing in autoclave	LWR	SS, Al, Mg, U-Mo, U-Nb
Energy Science Center	Scanning Electrochemical Cell Microscopy (SECCM)	N/A	Variety of materials capable of measuring electrochemical properties at fine scale
Environmental Molecular Sciences Laboratory	Scanning Kelvin Probe Force Microscopy	N/A	Variety of materials capable of measuring surface work function at fine scale
Applied Materials and Manufacturing Group	Coating Adhesion tests	N/A	Coated surfaces over structural materials

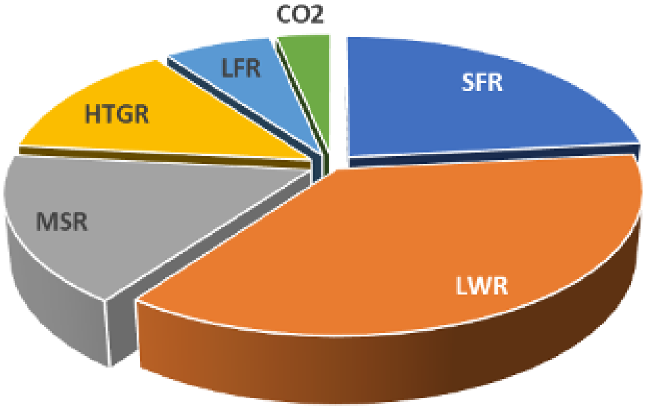

Figure 2. Reactor environments covered by reactor-specific testing capabilities available to AMMT.

The testing capabilities for evaluating the synergistic effects of mechanical loading and irradiation on corrosion performance are also evaluated. As shown in Table 7, the first two columns on the left define the corrosion system with the material and environment information. The materials are divided into two categories, unirradiated and irradiated, to separate the impact of irradiated microstructure on corrosion. The synergistic effects of stress and irradiation are represented with the rest of the columns in the table. The cells populated with plus (+) signs are the available testing capabilities. The number of plus signs qualitatively represents the readiness (or accessibility) of a testing capability. More plus signs qualitatively indicate more readily available testing capability. As we can see from the column indicating unloaded specimens, the ranking of the readiness for different test environment matches the finding in Fig. 2 without considering synergistic effects. As expected, the readiness of irradiated testing capabilities is much less than that of unirradiated testing capabilities.

Testing capabilities with either static or dynamic loading are readily available for water environments thanks to extensive research activities on SCC and corrosion fatigue across multiple laboratories. However, testing capabilities to assess the synergy between stress and corrosion is not available for other advanced reactor environments except for helium. The situation is even worse for testing irradiated materials due to the challenges of handling radioactive materials.

For the synergistic effects between radiation and corrosion, the testing capability is also very limited. In situ irradiation capability exists for water and molten salt environments, but with very limited capacity. Conversely, the effect of irradiation on the environment of liquid sodium or helium would be negligible. Any synergistic effect between irradiation and corrosion in these systems would manifest through dynamic interaction inside the material, rather than in the corrosive environment. As a result, an *in situ* irradiation capability may not be important for

Table 7. Readiness of testing capabilities for evaluating synergistic effects of mechanical stress and irradiation on corrosion.

Corrosion system		**Testing capability**				
Material	**Reactor environment**	**With mechanical stress**			**With *in situ* irradiation**	
		No load	Static load	Dynamic load	Ions	Gamma/neutrons
Unirradiated materials	Water	++++	+++	+++	+	
	Molten salt	++				+
	Sodium	+++				
	Helium	+	+			
Irradiated materials (radioactive)	Water	+++	++	++	+	
	Molten salt	+				+
	Sodium					
	Helium		+			

these corrosion systems.

6.3 Summary and Conclusions

Overall, there are sufficient testing capabilities available across the national laboratories to meet the corrosion testing needs of AMMT. There are more testing capabilities available for current LWR environments compared to advanced reactor types such as sodium fast reactors (SFRs) and MSRs. There is a need to develop corrosion experiment capabilities in testing irradiated, radioactive materials if the irradiated microstructure is deemed to be a critical factor influencing the corrosion behavior. *in situ* irradiation capability to emulate the synergy between irradiation damage and corrosion attack is available for LWRs, but is very limited for other reactor coolant environments.

7. SUGGESTED PATH FORWARD FOR ADVANCED MATERIALS MANUFACTURING TECHNOLOGIES CORROSION PROGRAM

The Advanced Materials Manufacturing Technologies (AMMT) program has developed a corrosion study strategy for fiscal years 2024–2026. Corrosion is a vast research area, and the research effort must be focused and application-specific. This requires a clear identification of the corrosion systems of interest (i.e., the material-environment combination) and the synergistic effects with other degradation mechanisms encountered in service. Due to the vast space of possible corrosion studies and the limits on available resources for study, including facilities and testing methods, prioritization must occur. Thus, the AMMT program will initially focus on the experimental characterization of additively manufactured (AM) 316H corrosion by molten chlorides and liquid sodium. With additional time and resource availability, molten fluorides, high temperature helium, liquid lead, and other advanced reactor environments will be studied, in that order of priority. Corrosion testing of additional materials will also be considered as they are developed and rise in priority. Corrosion issues unique to light water reactor (LWR) environments will not be studied unless a specific need or directive arises due to being studied within other DOE Office of Nuclear Energy (DOE-NE) programs, such as the Light Water Reactor Sustainability program. Advanced modeling and simulation may be introduced into the program if a specific need arises; however, given the complexity of AM material microstructures and its interplay with corrosion mechanisms, an experimental campaign is initially recommended.

In general, the testing of unirradiated specimens outside of a neutron-irradiation environment is recommended as the first step in testing AM components for reactor applications. This is due to cost and time involved with testing irradiated materials or performing *in situ* irradiation testing. Laboratory testing of unirradiated specimens can answer questions regarding the impact of process variability, post-build treatment, surface finish, and corrosion mechanisms. The second stage of corrosion testing for reactor environments can entail irradiated AM materials tested in the laboratory to determine the impact of irradiation-driven microstructural changes on corrosion behavior. Irradiation-driven microstructural changes may be the major driver of irradiation effects on corrosion behavior when the service temperature is elevated sufficiently for rapid defect migration, as in the case of many advanced reactor designs. At lower temperatures, defect production rates may be important. Finally, *in situ* corrosion testing in a reactor may be possible (depending on the availability of test capabilities or surveillance specimens in as-built reactors) for fully prototypical testing, which can account for irradiation-induced chemistry changes in the coolant, actual coolant flow rates, etc.

Given the features of AM materials (surface roughness, solute segregation, complex microstructure, and residual stresses), some amount of post-build processing generally occurs. The surface may be machined, as previously discussed. Post-build heat treatment is also common for stress relief, solution annealing, or microstructure homogenization [4]. Furthermore, a material may be processed to optimize its structure for one particular property (e.g., creep strength), which may impact its corrosion behavior. As a result, the corrosion behavior should be assessed for each instantiation of the AM-built and post-processed material. This will reveal how microstructure tuning for a given property and component performance will affect the corrosion behavior.

Corrosion testing will focus on both characterizing phenomena of engineering interest, such as as weight loss/gain, pit and crevice formation, and mechanical response after corrosion, as well as understanding corrosion mechanisms at the mesoscale, such as characterization of phases induced by corrosion and local chemistry changes. The specific corrosion testing strategy employed to assess an AM material for a reactor environment will depend upon the degree of prior knowledge about the behavior of the material composition in the environment. For example, if prior information exists for conventionally manufactured 316H in FLiNaK [75], then the corrosion testing strategy can leverage this prior knowledge to its advantage to rank specific corrosion tests by estimated likelihood of importance for the material. As a result, a mass transfer test in a flowing salt loop would be a high-priority test. If, however, little or no information exists, then a rapid assessment campaign of static coupon tests may help gain a sense of how the material performs so additional specific tests can be selected. If a material-environment system is chemically complex and not well understood (such as corrosion in molten chloride systems), determination of corrosion species is needed to identify the surface sites most vulnerable to specific species attack as well as to establish which grain, chemical composition, and microstructure may provide best the corrosion resistance.

Some evidence indicates that as-fabricated, net-shape AM 316 components may have improved corrosion behavior over wrought 316 stainless steel (SS) due to the surface roughness; however, other evidence exists that rough surfaces increase crevice corrosion. Because AM components may be deployed without further surface finishing, understanding the effect of the surface on corrosion behavior is crucial. Weight measurements as well as microstructure and microchemical evolution at the surface are needed. Build porosity is also a concern, as is the presence of oxide phases or atypical inclusions and residual stresses. Given the likelihood of crevice corrosion at the as-built surface, three-dimensional, non-destructive examination before and after corrosion testing is recommended, such as X-ray computed tomography, which will allow for characterization of comparative pre- and post-corrosion porosity at the surface and within the same sample. Upon identification of areas of interest, these specimens can then be sectioned to study microstructure and local composition variation with scanning electron microscopy and transmission electron microscopy imaging.

Conversely, as-built specimens finished to a smooth surface may be useful to assess underlying corrosion mechanisms and understand the extent to which corrosion is localized to or affected by the rough surface. Thus, a given material should be tested with both the rough surface and a polished surface; this is hereafter referred to as the “two-surface test.” The corrosion assessment may also include conventionally manufactured (e.g., wrought) smooth specimens of the same composition. This is of particular interest if AM processing is being proposed to replace conventional fabrication of a material currently in service. Similarly, the effect of post-build heat treatments can also be assessed via the two-surface test. The two-surface test strategy is applicable to a variety of tests, such as static corrosion tests, flow tests, and stress corrosion cracking studies.

The impact of AM build process variability on AM material properties is a significant concern and extends to their corrosion behavior. In this context, process variability refers to variations in the as-built microstructure from a single, specific machine. Even with the same build parameters in the same AM machine (e.g., laser power, scan pattern, and speed for laser powder bed fusion), sources of process variability include the laser power and scan speed; feedstock lots; atmospheric storage condition of the feedstock, especially powder feedstock; atmospheric composition during the build, including humidity levels [74]; and heat dissipation during the build as a result of build plate heating, surrounding atmosphere, and build geometry.

Process variability should be addressed with a combination of experiments and data analytics. Variability should be considered at the microscale and the macroscale. At the microscale, the statistical distribution of a corrosion behavior of interest should be understood with respect to key microstructural features. Successful assessment of the impact of process variability on corrosion behavior requires data traceability linking sources of process variability (e.g., build parameters, feedstock properties) and microstructure statistics (grain geometries, dislocation cell characteristics, solute distribution) to the corrosion test results. Conversely, macroscale variability can be tested by taking samples from different locations within a component.

In addition, the geometry of the as-built specimen from which corrosion samples are removed should be considered as part of process variability. It is conceivable to take corrosion specimens from small specimens with limited build volume, while the actual component will be larger. Given the impact of build volume on thermal history and the resulting microstructure, corrosion specimens sectioned from specimens of representative geometries and volumes of the actual component may also need to be assessed.

For maximum impact, the materials tested within the AMMT corrosion campaign must be the same as the materials employed within the neutron irradiation, ion irradiation, and rapid qualification testing. The material condition includes the feedstock source, contamination (e.g., with oxygen), build parameters, and post-build treatments including surface finishing and annealing. Coordination is required across program areas to ensure sufficient material with a fully traceable pedigree is available for testing. By evaluating pedigreed materials for their corrosion performance, corrosion testing will be an integrated part of the AMMT experimental campaign.

REFERENCES

[1] M. Li, D. Andersson, R. Dehoff, A. Jokisaari, I. V. Rooyen, D. Cairns-Gallimore, Advanced Materials and Manufacturing Technologies (AMMT) 2022 Roadmap, Tech. Rep. ANL-23/12, Argonne National Laboratory (September 2022).

[2] A. Vafadar, F. Guzzomi, A. Rassau, K. Hayward, Advances in metal additive manufacturing: A review of common processes, industrial applications, and current challenges, Applied Sciences 11 (2021) 1213.

[3] G. Liu, X. Zhang, X. Chen, Y. He, L. Cheng, M. Huo, H. Yin, F. Hao, S. Chen, P. Wang, S. Yi, L. Wan, Z. Mao, Z. Chen, X. Wang, Z. Cao, J. Lu, Additive manufacturing of structural materials, Materials Science & Engineering R 145 (2021) 100596.

[4] T. Wohlers, I. Campbell, O. Diegel, R. Huff, J. Kowen, 3D printing and additive manufacturing state of the industry, Tech. rep., Lund University, Lund, Sweden (2017).

[5] R. Russell, D. Wells, J. Waller, B. Poorganji, E. Ott, T. Nakagawa, H. Sandoval, N. Shamsaei, M. Seifi, Qualification and certification of metal additive manufactured hardware for aerospace applications, in: Additive Manufacturing for the Aerospace Industry, Elsevier, Amsterdam, The Netherlands, 2019.

[6] Wilmoth, R and Nguyen, J and Schaeffer, J B and Douglass, D M, Additive manufacturing in a naval aircraft carrier construction project, `https://amfg.ai/2019/10/08/10-of-the-biggest-challenges-in-scaling-additive-manufacturing-for-production-expert-roundup/` (2023).

[7] Nuclear Energy Institute, Roadmap for regulatory acceptance of advanced manufacturing methods in the nuclear energy industry, May 13, 2019 (2019).

[8] R. B. Rebak, X. Lou, Environmental cracking and irradiation resistant stainless steels by additive manufacturing, Technical report, GE Global Research (March 2018).

[9] D. W. Gandy, Strategy and approach for qualification of nuclear components produced via additive manufacturing, in: US DOE Advanced Methods of Manufacturing Workshop, US Department of Energy, Germantown, MD, USA, 2016.

[10] X. Lou, M. Song, P. W. Emigh, M. A. Othon, P. L. Andresen, On the stress corrosion crack growth behavior in high temperature water of 316L stainless steel made by laser powder bed fusion additive manufacturing, Corrosion Science 128 (2017) 140–153.

[11] B. Alexandreanu, X. Zhang, Y. Chen, W.-Y. Chen, M. Li, Mechanical testing of additively manufactured materials, Tech. Rep. ANL/NSE-22/83, Argonne National Laboratory (2022).

[12] M. D. Shamsujjoha, S. R. Agnew, J. M. Fitz-gerald, W. R. Moore, T. A. Newman, High strength and ductility of additively manufactured 316L stainless steel explained, Metallurgical and Materials Transactions A 49 (A) (2018) 3011.

[13] M. Li, X. Zhang, W.-Y. Chen, T. S. Byun, Creep behavior of 316L stainless steel manufactured by laser powder bed fusion, Journal of Nuclear Materials 548 (2021) 152847.

[14] U.S. Nuclear Regulatory Commission, Action plan for advanced manufacturing technologies, Revision 1, Tech. Rep. ML19333B980, U.S. Nuclear Regulatory Commission, Washington, DC (2020).

[15] J. Simpson, J. Haley, C. Cramer, O. Shafer, A. Elliott, W. Peter, L. Love, R. Dehoff, Considerations for application of additive manufacturing to nuclear reactor core components, Tech. rep., ORNL/TM-2019/1190, M3CT-19OR06090123 (2019).

[16] X. Zhang, F. Liou, Chapter 1: Introduction to additive manufacturing, in: J. Pou, A. Riveriro, J. P. Davim (Eds.), Handbooks in Advanced Manufacturing-Additive Manufacturing, Elsevier Inc, 2021, pp. 1–31.

[17] I. Gibson, D. Rosen, B. Stucker, M. Khorasani, I. Gibson, D. Rosen, B. Stucker, M. Khorasani, Materials for additive manufacturing, Springer, Cham, Switzerland, 2021.

[18] T. DebRoy, H. Wei, J. Zuback, T. Mukherjee, J. Elmer, J. Milewski, A. M. Beese, A. d. Wilson-Heid, A. De, W. Zhang, Additive manufacturing of metallic components–process, structure and properties, Progress in Materials Science 92 (2018) 112–224.

[19] C. Örnek, Additive manufacturing – a general corrosion perspective, Corrosion Engineering, Science and Technology 53 (7) (2018) 531–535.

[20] E. J. Schindelholz, M. A. Melia, J. M. Rodelas, Corrosion of additively manufactured stainless steels—process, structure, performance: A review, Corrosion 77 (5) (2021) 484–503.

[21] G. Sander, J. Tan, P. Balan, O. Gharbi, D. R. Feenstra, L. Singer, S. Thomas, R. G. Kelly, J. R. Scully, N. Birbilis, Corrosion of additively manufactured alloys: A review, Corrosion 74 (12) (2018) 1318.

[22] K. Sridharan, T. Allen, Corrosion in molten salts, in: Molten salts chemistry, Elsevier, 2013, pp. 241–267.

[23] J. R. Davis, Corrosion: Understanding the Basics, ASM International, 2000.

[24] R. I. Revilla, M. Van Calster, M. Raes, G. Arroud, F. Andreatta, L. Pyl, P. Guillaume, I. De Graeve, Microstructure and corrosion behavior of 316L stainless steel prepared using different additive manufacturing methods: A comparative study bringing insights into the impact of microstructure on their passivity, Corrosion Science 176 (2020) 108914.

[25] M. A. Melia, H.-D. A. Nguyen, J. M. Rodelas, E. J. Schindelholz, Corrosion properties of 304L stainless steel made by directed energy deposition additive manufacturing, Corrosion Science 152 (2019) 20–30.

[26] J. Yang, L. Hawkins, L. He, S. Mahmood, M. Song, K. Schulze, X. Lou, Intragranular irradiation-assisted stress corrosion cracking (IASCC) of 316L stainless steel made by laser direct energy deposition additive manufacturing: Delta ferrite-dislocation channel interaction, Journal of Nuclear Materials 577 (2023) 154305.

[27] C. Wang, P. Zhu, F. Wang, Y. Lu, T. Shoji, Anisotropy of microstructure and corrosion resistance of 316L stainless steel fabricated by wire and arc additive manufacturing, Corrosion Science 206 (2022) 110549.

[28] X. Chen, J. Li, X. Cheng, H. Wang, Z. Huang, Effect of heat treatment on microstructure, mechanical and corrosion properties of austenitic stainless steel 316L using arc additive manufacturing, Materials Science and Engineering: A 715 (2018) 307–314.

[29] G. Ko, W. Kim, K. Kwon, T.-K. Lee, The corrosion of stainless steel made by additive manufacturing: A review, Metals 11 (3) (2021) 516.

[30] T. Voisin, R. Shi, Y. Zhu, Z. Qi, M. Wu, S. Sen-Britain, Y. Zhang, S. Qiu, Y. Wang, S. Thomas, et al., Pitting corrosion in 316L stainless steel fabricated by laser powder bed fusion additive manufacturing: A review and perspective, JOM 74 (4) (2022) 1668–1689.

[31] I. Segura, L. Murr, C. Terrazas, D. Bermudez, J. Mireles, V. Injeti, K. Li, B. Yu, R. Misra, R. Wicker, Grain boundary and microstructure engineering of Inconel 690 cladding on stainless-steel 316L using electron-beam powder bed fusion additive manufacturing, Journal of Materials Science & Technology 35 (2) (2019) 351–367.

[32] M. N. Gussev, N. Sridharan, S. Babu, K. A. Terrani, Influence of neutron irradiation on Al-6061 alloy produced via ultrasonic additive manufacturing, Journal of Nuclear Materials 550 (2021) 152939.

[33] MCB Issue List Regarding APR-1400, FSAR Section 5.4.2.1.

[34] W. J. Shack, T. F. Kassner, P. S. Maiya, J. Y. Park, W. E. Ruther, BWR pipe crack and weld overlay studies, Nuclear Engineering and Design 89 (2-3) (1985) 295.

[35] F. Ford, P. Andresen, Development and use of a predictive model of crack propagation in 304/316L, A533B/A508 and Inconel 600/182 alloys in 288 C water, in: Proceedings of the third international symposium on environmental degradation of materials in nuclear power systems, 1988.

[36] B. Arsenault, E. Ghali, Stress corrosion cracking of pressure vessel welded carbon steels, International Journal of Pressure Vessels and Piping 45 (1) (1991) 23–41.

[37] G. S. Was, Recent developments in understanding irradiation assisted stress corrsion cracking, in: Proceedings of the 11th International Conference on Environmental Degradation of Materials in Nuclear Power Systems-Water Reactors, Stevenson, Washington, Aug. 10-14, 2003, Am. Nucl. Soc., 2003.

[38] P. Scott, M. Le Calver, Some possible mechanisms of intergranular stress corrosion cracking of Alloy 600 in PWR primary water, in: Proceedings of the sixth international symposium on environmental degradation of materials in nuclear power systems-water reactors, 1993.

[39] A. Hirano, K. Sakaguchi, T. Shoji, Effects of water flow rate on fatigue life of structural steels under simulated BWR environment, in: ASME Pressure Vessels and Piping Conference, Vol. 42797, 2007, pp. 231–242.

[40] S. S. Raiman, S. Lee, Aggregation and data analysis of corrosion studies in molten chloride and fluoride salts, Journal of Nuclear Materials 511 (2018) 523–535.

[41] J. Zhang, C. W. Forsberg, et al., Redox potential control in molten salt systems for corrosion mitigation, Corrosion Science 144 (2018) 44–53.

[42] K. Aoto, P. Dufour, Y. Hongyi, J. P. Glatz, Y.-i. Kim, Y. Ashurko, R. Hill, N. Uto, A summary of sodium-cooled fast reactor development, Progress in Nuclear Energy 77 (2014) 247–265.

[43] M. Li, K. Natesan, W.-Y. Chen, Material performance in sodium, in: Comprehensive Nuclear Materials 2nd Edition, Vol. 4, Elsevier, Oxford, 2020, pp. 339–356.

[44] E. Yoshida, S. Kato, Sodium compatibility of ODS steel at elevated temperature, Journal of nuclear materials 329 (2004) 1393–1397.

[45] E. Yoshida, T. Furukawa, Corrosion issues in sodium-cooled fast reactor (SFR) systems, in: Nuclear Corrosion Science and Engineering, Elsevier, 2012, pp. 773–806.

[46] O. Sreedharan, B. Madan, J. Gnanamoorthy, Threshold oxygen levels in Na (I) for the formation of $NaCrO_2$ (s) on 18-8 stainless steels from accurate thermodynamic measurements, Journal of Nuclear Materials 119 (2-3) (1983) 296–300.

[47] M. O. Rothwell, Cold trap performance: a general analysis, Ph.D. thesis, Oregon State University (1972).

[48] G. S. Was, T. R. Allen, Corrosion issues in current and next-generation nuclear reactors, Structural Alloys for Nuclear Energy Applications (2019) 211–246.

[49] C. Schroer, O. Wedemeyer, J. Konys, Aspects of minimizing steel corrosion in liquid lead-alloys by addition of oxygen, in: International Conference on Nuclear Engineering, Vol. 49330, 2010, pp. 207–218.

[50] X. Gong, R. Li, M. Sun, Q. Ren, T. Liu, M. P. Short, Opportunities for the LWR ATF materials development program to contribute to the LBE-cooled ADS materials qualification program, Journal of Nuclear Materials 482 (2016) 218–228.

[51] R. Quade, A. McMain, Hydrogen production with a high-temperature gas-cooled reactor (HTGR), in: Hydrogen Energy: Part A, Springer, 1975, pp. 137–154.

[52] D. Kumar, R. R. Adharapurapu, T. M. Pollock, G. S. Was, High-temperature oxidation of Alloy 617 in helium containing part-per-million levels of CO and CO_2 as impurities, Metallurgical and Materials Transactions A 42 (2011) 1245–1265.

[53] E. M. Hussein, Emerging small modular nuclear power reactors: A critical review, Physics Open 5 (2020) 100038.

[54] G. S. Was, D. Petti, S. Ukai, S. Zinkle, Materials for future nuclear energy systems, Journal of Nuclear Materials 527 (2019) 151837. `doi:10.1016/j.jnucmat.2019.151837`.

[55] N. D. B. Ezell, S. S. Raiman, J. M. Kurley, J. McDuffee, Neutron irradiation of Alloy N and 316L stainless steel in contact with a molten chloride salt, Nuclear Engineering and Technology 53 (3) (2021) 920–926.

[56] F. Schmidt, P. Hosemann, R. O. Scarlat, D. K. Schreiber, J. R. Scully, B. P. Uberuaga, Effects of radiation-induced defects on corrosion, Annual Review of Materials Research 51 (2021) 293–328.

[57] W. Zhou, Y. Yang, G. Zheng, K. B. Woller, P. W. Stahle, A. M. Minor, M. P. Short, Proton irradiation-decelerated intergranular corrosion of Ni-Cr alloys in molten salt, Nature communications 11 (1) (2020) 3430.

[58] P. Okamoto, L. Rehn, Radiation-induced segregation in binary and ternary alloys, Journal of Nuclear Materials 83 (1) (1979) 2–23.

[59] J. Stiegler, L. Mansur, Radiation effects in structural materials, Annual review of materials science 9 (1) (1979) 405–454.

[60] P. Scott, A review of irradiation assisted stress corrosion cracking, Journal of nuclear materials 211 (2) (1994) 101–122.

[61] N. AlMousa, W. Zhou, K. B. Woller, M. P. Short, Effects of simultaneous proton irradiation on the corrosion of commercial alloys in molten fluoride salt, Corrosion Science 217 (2023) 111154.

[62] X. Zhang, X. Zhou, T. Hashimoto, L. Bin, Localized corrosion in AA2024-T351 aluminium alloy: Transition from intergranular corrosion to crystallographic pitting, Materials Characterization 130 (2017) 230–236.

[63] J. L. Bartlett, X. Li, An overview of residual stresses in metal powder bed fusion, Additive Manufacturing 27 (2019) 131–149.

[64] A. Sola, A. Nouri, Microstructural porosity in additive manufacturing: The formation and detection of pores in metal parts fabricated by powder bed fusion, Journal of Advanced Manufacturing and Processing 1 (3) (2019) e10021.

[65] H. L. Wei, J. Mazumder, T. DebRoy, Evolution of solidification texture during additive manufacturing, Scientific Reports 5 (2015) 16446.

[66] G. Sander, S. Thomas, V. Cruz, M. Jurg, N. Birbilis, X. Gao, M. Brameld, C. Hutchinson, On the corrosion and metastable pitting characteristics of 316L stainless steel produced by selective laser melting, Journal of the electrochemical society 164 (6) (2017) C250.

[67] X. Lou, P. L. Andresen, R. B. Rebak, Oxide inclusions in laser additive manufactured stainless steel and their effects on impact toughness and stress corrosion cracking behavior, Journal of Nuclear Materials 499 (2018) 182–190.

[68] C. Man, C. Dong, T. Liu, D. Kong, D. Wang, X. Li, The enhancement of microstructure on the passive and pitting behaviors of selective laser melting 316L stainless steel in simulated body fluid, Applied Surface Science 467 (2019) 193–205.

[69] R. F. Schaller, A. Mishra, J. M. Rodelas, J. M. Taylor, E. J. Schindelholz, The role of microstructure and surface finish on the corrosion of selective laser melted 304, Journal of the Electrochemical Society 165 (5) (2018) C234.

[70] Y. Nakao, K. Nishimoto, Effects of laser surface melting on steel and nickel-base alloy clad corrosion resistance of stainless layers in cast bimetallic pipes, ISIJ International 33 (9) (1993) 934–940.

[71] D. Kong, C. Dong, X. Ni, L. Zhang, H. Luo, R. Li, L. Wang, C. Man, X. Li, Superior resistance to hydrogen damage for selective laser melted 316L stainless steel in a proton exchange membrane fuel cell environment, Corrosion Science 166 (2020) 108425.

[72] D. J. Sprouster, W. S. Cunningham, G. P. Halada, H. Yan, A. Pattammattel, X. Huang, D. Olds, M. Tilton, Y. S. Chu, E. Dooryhee, et al., Dislocation microstructure and its influence on corrosion behavior in laser additively manufactured 316L stainless steel, Additive Manufacturing 47 (2021) 102263.

[73] J. Bedmar, N. Abu-Warda, S. García-Rodríguez, B. Torres, J. Rams, Influence of the surface state on the corrosion behavior of the 316 L stainless steel manufactured by laser powder bed fusion, Corrosion Science 207 (2022) 110550.

[74] R. J. Hebert, Metallurgical aspects of powder bed metal additive manufacturing, Journal of Materials Science 51 (2016) 1165–1175.

[75] S. S. Raiman, J. M. Kurley, D. Sulejmanovic, A. Willoughby, S. Nelson, K. Mao, C. M. Parish, M. S. Greenwood, B. A. Pint, Corrosion of 316H stainless steel in flowing FLiNaK salt, Journal of Nuclear Materials 561 (2022) 153551.